8-2022

Cell-Free Dna Sequencing In Multiple Myeloma

Russell Irwin

Recommended Citation

Irwin, Russell, "Cell-Free Dna Sequencing In Multiple Myeloma" (2022). *Dissertations and Theses (Open Access)*. 1211.
https://digitalcommons.library.tmc.edu/utgsbs_dissertations/1211

Cell-free DNA Sequencing in Multiple Myeloma

by

Russell Mac Irwin, B.S.ASNR

APPROVED:

_____
Michael Green, Ph.D.
Advisory Professor

_____
Robert Orlowski, MD, Ph.D.

_____
Anirban Maitra, MBBS

_____
Michelle Hildebrandt, Ph.D.

_____
Michael Lorenz, Ph.D.

_____
Hans Lee, M.D.

APPROVED:

_____
Dean, The University of Texas

MD Anderson Cancer Center UTHealth Graduate School of Biomedical Sciences

Cell-free DNA Sequencing in Multiple Myeloma

A Thesis

Presented to the Faculty of:

The University of Texas

MD Anderson Cancer Center UTHealth

Graduate School of Biomedical Sciences

in Partial Fulfillment

of the Requirements

for the Degree of

Master of Science

by

Russell Mac Irwin, B.S.ASNR
Houston, Texas

August 2022

v

2   Abstract

Cell-free DNA Sequencing in Multiple Myeloma

Russell M. Irwin, BS.ASNR

Advisory Professor: Michael R. Green, PhD

Multiple myeloma (MM) is an incurable plasma cell dyscrasia. Recent advances in MM therapy, including CAR-T therapy, have increased survival and shown the value of assessing treatment response with great sensitivity, both in acute and long-term settings. Cell-free DNA, DNA fragments which are released into circulation as a part of normal cellular turnover, is a useful and dynamic biomarker in cancer patients due to the presence of circulating tumor DNA (ctDNA), which is readily identified using next generation sequencing. Here we report the analytical sensitivity, applicability, consistency, and prognostic ability of M5Seq, a novel hybrid capture panel designed for MM ctDNA. We performed in-silico validation of this panel and found high applicability (1,173/1,212 tumors with ≥1 variant covered, 97%, mode 6 variants covered). By sequencing serial dilutions of simulated cancer DNA in healthy donor DNA, we observed a limit of analytical sensitivity at 5×10^{-5} and a limit of linearity at 10^{-4}. Then, we applied this method to the matched pre-treatment tumor and plasma samples of 10 newly diagnosed MM patients. We observed moderate concordance in the mutations detected in each compartment, consistent with existing literature. Based off these data, we applied M5Seq to plasma samples from 18 patients undergoing anti-BCMA chimeric antigen receptor T cell therapy (CAR-T). We observed similar concordance in the CAR-T cohort as in the newly diagnosed patients. In 14 evaluable patients, we observed no statistically significant decreases in variant allele fraction

within two days of CAR-T infusion between patients achieving a complete response or better

within 30 days of infusion as determined by IMWG criteria, as compared to those patients

with stable or progressing disease. Furthermore, while we observed a slight overall survival

advantage in patients with decreased VAF from baseline, this association did not meet the

threshold for statistical significance.

3   <u>Table of Contents</u>

4 <u>List of Figures</u>

5 <u>List of Tables</u>

6   Introduction

6.1   Multiple myeloma etiology, biology, and treatment

Multiple myeloma (MM) is a malignancy of differentiated, mature lymphoid-derived plasma cells which presents most often in patients over the age of 50[1]. MM occurs at an age-adjusted frequency of 4.3 per 100,000 in the United States, with greater frequency in African Americans than other ethnic groups, and with greater frequency in men than women[2]. The average age of onset for MM is 66 years[3].

MM is characterized by genetic heterogeneity, mutational burden, and high-risk genomic lesions including t(4;14) 14q32, del(17p) and del(13q) [4-7]; hyperdiploidies presenting as trisomies in odd-numbered chromosomes are also common. Plasma cells, having undergone multiple rounds of somatic hypermutation and class-switch recombination, frequently see off-target single nucleotide variants (SNVs) and indels characteristic of cytosine deaminase activity in B cell malignancies, such as in *Bcl6, Cd19, Cd83, Pax5,* and *Bcl11*[8, 9].

Plasma cells are characteristic in that they are antibody-secreting cells, and because multiple myeloma tumor cells are typically derived from the same clone, they all secrete the same antibody. This antibody is detectable via serum protein electrophoresis and immunofixation and is used as a primary biomarker, known as the M (myeloma) protein[10]. In addition, many tumors secrete excess free light chain, disrupting the normal ratio of κ isotype free light chains in serum to λ free light chains. The serum free light chain (sFLC) ratio is also an important metric of performance[11].

Frontline treatment for MM is based on autologous stem cell transplant (ASCT) and alkylating chemotherapy, bookended by combination therapies of steroids, proteasome

inhibitors, and immunomodulatory agents. In the last 15 years, the introduction of novel therapeutics such as bortezomib and other proteasome checkpoint inhibitors has dramatically improved overall survival (OS) and progression-free survival (PFS) in patients who respond well to first-line treatments[12].

This increased survival has exposed a weakness in the traditional histopathology- and protein-based definitions of complete response (CR) and stringent complete response (sCR), which are now inadequate for predicting survival[13].

6.1.1 Chimeric antigen receptor T-Cell therapy

Another major development in MM therapy is the recent FDA approval of chimeric antigen receptor T-cells (CAR-T) targeting B cell maturation antigen (BCMA), ABECMA (idecabtagene vicleucel, ide-cel) in 2020[14] and CARVYKTI (ciltacabtagene autoleucel, cilta-cel) in 2022. Both treatments utilize patient-derived CD8+ T-cells transfected with vector coding for the second-generation chimeric antigen receptor construct, including a BCMA-specific short chain variable fragment (scFv), 4-1BB costimulatory domain, and CD3ζ signaling domain. These cells are expanded *ex vivo*. The patient then undergoes lymphodepleting chemotherapy before cell reinfusion.

Results of the initial KarMMa trial of ide-cel indicate an 85% overall response rate and a 45% complete response rate. However, within six months of infusion, 40% of complete responders experienced a relapse, and median progression-free survival was 11.8 months[15]. Similarly, the CARTITUDE-1 trial of cilta-cel demonstrated 97% overall response rate and 67% of patients achieved sCR, and 12-month PFS was 77%[16]. At this time, anti-BCMA CAR-T is only approved for patients with multiple-refractory MM. Due to the rate of relapse in CAR-T therapy, especially in ide-cel, novel strategies are necessary to

2

stratify patients by risk before CAR-T therapy and assess response kinetics

contemporaneously with the infusion in order to predict the likelihood of relapse.

6.2   Minimal residual disease: a cellular approach

Disease response kinetics in the context of CAR-T therapy are difficult to assess due

to the rapidity with which the therapy can effect a stringent complete response (sCR), defined

by the International Myeloma Working Group (IMWG) as absence of tumor cells in a

primary tumor sample as detected by immunofluorescence and a normal sFLC ratio. sCR is

often achieved within one month of CAR-T infusion, indicating that the tumor is killed

rapidly within the early days surrounding infusion. However, the actual tumor burden is

difficult to define during this window for a number of reasons. First and foremost, blood-

based assays for assessing disease burden in MM have traditionally lacked the sensitivity to

detect low-level disease burden at levels comparable to or exceeding the equivalent disease

burden of a sCR. The ability of a patient to relapse after achieving sCR indicates that some

minimal residual disease (MRD) is still present beyond the level of detection achievable via

immunofluorescence and sFLC assays.

MRD is a much stronger predictor of progression free and overall survival than sCR

alone [13, 17, 18], whether detected by next-generation multicolor flow cytometry

(MFC)[17, 19-22] or molecular methods [18, 23, 24]. Recent meta-analyses of MM studies

have shown that compared to MRD+ patients, MRD- patients have dramatically lower hazard

ratios regardless of disease stage, MRD measurement method and sensitivity, cytogenetic

risk factors, disease setting (newly diagnosed vs relapse, transplant eligible vs not), and depth

of clinical response, including achievement of CR or sCR [25].

6.2.1 Multicolor flow cytometry and its use in assessing minimal residual disease

Due to several commonalities between MM and other plasma cell dyscrasias such as diffuse large B-cell lymphoma and chronic lymphocytic leukemia, it is often useful to apply techniques developed for other cancers such as V(D)J sequencing[23] and multicolor flow cytometry (MFC)-based MRD detection[26, 27] to MM. MFC is the diagnostic gold standard for assessing immunophenotypic MRD due to its high sensitivity and applicability. Next generation multicolor/multiparameter flow cytometry has sensitivity on the order of 1×10^{-6}; older MFC technologies retain sensitivity on the order of 1×10^{-4}-1×10^{-5} [17]. Even this lower level of sensitivity can be used to inform treatment decisions [17], and a failure to detect MRD at this level of sensitivity is a strong prognosticator of OS and PFS[18, 22].

Flow cytometry has been in use for MRD assessment in clinics for over two decades[26] and improvements in technique have caused sensitivity to increase from 10^{-4}, using the original CD45/CD38/CD138 panel (or an alternative to CD138, up to three colors total), to 10^{-6} in some modern versions of the assay utilizing up to 10 colors. Use of MFC in the GEM2000 trial showed definitively the survival benefit of MRD negativity by MFC[28]. In agreement with early literature, Paiva *et al* showed that MRD negativity is a better predictor of PFS and OS than immunofixation or CR with sensitivity of 10^{-4}, and posited that greater sensitivity might allow MFC to rival PCR-based methods. Sensitivity advances in MFC have allowed for comparison of benefits for various sensitivity levels: Rawstron *et al* showed that there is a comparative benefit per log reduction of sensitivity, correlating to an extra year, on average, of OS per log reduction[17]. MRD detection is considered a secondary clinical endpoint for trials, such as the PETHEMA/GEM2012/MENOS65 trial which has incorporated NGF as the primary MFC protocol[22].

Various facilities have their own protocols and panels for MFC detection of MRD, which may use multiple tubes and 8-10 colors for immunophenotyping. Standard of care methods include the EuroFlow-based eight color, two-tube panel[29] and some ten-color panels[30], offering sensitivity down to $2x10^{-6}$ to $6x10^{-6}$, respectively. In general, at least seven colors are required to give optimal sensitivity and provide comparable results, allowing for standardization between facilities[31], but standardization is still a challenge and efforts to remedy this are ongoing[32]. Another major challenge to MFC-based MRD detection is the nature of the sample required. A BMB aspirate consists of living cells, so the processing time between aspiration time and analysis must be as short as possible to obtain the most comprehensive results.

6.2.2   Tumor infiltration and extramedullary disease

Plasma cells reside in their niche in the bone marrow but can, and frequently do, migrate throughout the bone marrow and through the entire lymphatic system. Myeloma cells can form tumors distant from the original tumor site, creating a patchy pattern in the bone marrow, and causing extramedullary disease in the skull, sternum, lumbar spine, and elsewhere. Plasmacytomas are identified using MRI or x-ray magnetic bone imaging (MBI), which have been standard practice in MM diagnosis and treatment for decades[33]. The disappearance of plasmacytomas identified at diagnosis via MRI or MBI is included in the IMWG definition of complete response and strict complete response[20]. Importantly, however, extramedullary plasmacytomas can serve as reservoirs for relapse.

In the last decade, [18]fluorodeoxyglucose positron emission tomography/computed tomography (FDG-PET/CT) has been demonstrated to be an impactful tool for predicting survival in newly-diagnosed patients by assessing disease burden, and showed some promise

in predicting outcomes based on response to ASCT[34-36] and anthracycline-based chemotherapy[37].The identification of extramedullary lesions with high standardized uptake values on FDG-PET/CT correlates with worse OS, but does not correlate with M protein levels [38]. FDG-PET/CT evaluation can be used to target certain regions for BMB beyond the standard iliac crest site and is used to determine whether ASCT has been effective, and patients who are FDG-PET/CT negative after ASCT are known to have longer PFS and OS than those patients who are FDG-PET/CT positive, regardless of CR status[39]. However, FDG-PET/CT is not effective in identifying diffuse bone marrow involvement[40], and only has moderate sensitivity and specificity for detecting lesions after treatment[41]. This would indicate that FDG-PET/CT lacks the necessary sensitivity to detect clonal cells which constitute a reservoir for relapse.

6.2.3   Circulating tumor cells: an alternative compartment

Circulating tumor cells (CTC) are plasma cells which are shed into the bloodstream and may be indicative of the primary tumor or an extramedullary tumor, and may be identified through MFC, PCR, or sequencing of peripheral blood mononuclear cells[42]. No matter which method is used, the obvious benefit to using this source is its ready availability and utility. Identification, isolation, and investigation of CTC can also be done by paramagnetic bead enrichment or microfluidic methods[43], and the genetic material from these cells is useful for downstream karyotypic, genetic, or genomic analysis such as PCR-based MRD detection[43-45]. CTC are not perfectly identical to primary tumor plasma cells: CTC adopt a quiescent phenotype and often display genetic features consistent with subclonality[45, 46]. That said, there is generally good overlap between CTC and primary tumor plasma cells[47].

As a part of the PETHEMA trials, Sanoja-Flores *et al* showed that the failure to detect CTC via NGF may lead to false negatives when compared to contemporaneous BM samples, but may also detect extramedullary disease, and that CTC identification is an independent predictor of PFS with a higher hazard ratio than BM MRD positivity, suggesting that the detection of CTC indicates increased tumor burden and/or extramedullary disease[48], and corroborating their earlier report that CTC levels indicate increased risk for MGUS and SMM patients[49]. This is in agreement with another report that >100 CTC in a sample on 150,000 PBMCs is an independent risk predictor[50], and a separate report that detection of CTC immediately before ASCT is an independent negative predictor of OS and PFS[51]. Taken together, the literature suggests that the presence of these cells, though somewhat rare outside of active disease, can serve indirect measurements of tumor burden.

6.3   Molecular alternatives to NGF/MFC MRD detection

The legacy alternative to MFC/NGF for MRD detection is allele-specific oligonucleotide quantitative PCR (ASO-qPCR), which has been validated to have comparable clinical significance at comparable levels of MRD detection to MFC-based MRD[52]. The principle of all approved ASO-qPCR and all approved NGS assays is the detection of clonotypic sequences in the rearranged V(D)J region of the clonal plasma cell genome; however, this is also a major flaw, as a minority of patients have no trackable gene rearrangement. NGS applicability is approximately 90%[53], while ASO-qPCR applicability is <80% and requires a complex workflow, including patient-specific primer design and manufacturing, germline Sanger sequencing, and the creation of a standard curve[54-56]. Digital droplet PCR (ddPCR), an evolution of qPCR, offers higher sensitivity and decreased workloads at the lab bench by eliminating the need for a standard curve, but still requires all

the other steps mentioned for ASO-qPCR. The technique has been shown to have comparable

sensitivity and specificity to ASO-qPCR[57], and has been validated by direct comparison to

NGS and ASO-qPCR in patients following ASCT[58].

Separately, liquid chromatography tandem mass spectrometry (LC-MS) platforms

have been tested for use in MRD detection with a focus on clonal M-protein detection in

serum, based on M-protein isoforms predicted by genomic data[59]. This is an evolution of

the traditional serum protein electrophoresis and immunofixation electrophoresis, which has

been used to quantify serum and urine M-protein for decades. Others have proposed the use

of MALDI-TOF MS to analyze M-protein levels and clonotypes[60, 61], and have

demonstrated the utility of this approach despite potential interference from monoclonal

antibody therapy; and Eveillard *et al* [62] showed that there was some agreement between the

MALDI-TOF method and MFC. The MS-based approaches tend to separate into two groups:

those using a mass-based approach, [63]; and those seeking specific clonotype sequences

after trypsin digestion[61, 64]. The IMWG has endorsed MS as an alternative to

immunofixation[65] and called for its inclusion in further clinical trials. One promising

report has demonstrated the use of DNA aptamers and a photometric assay in detecting

clonal IgG in serum at levels below the limit of IFE detection in a patient showing a

complete response and MRD negativity (at 10^{-5} by MFC) who later relapsed [66]. Others

have shown that MS can detect minimal residual disease (in the form of clonal M protein) in

sCR[67]. Finally, a group has shown that MRD+ status by LC-MS (using the clonotypic

approach) correlates with inferior survival, even when MRD negativity by sequencing is

achieved[68]. While these reports are promising, comparison to other MRD detection

techniques is needed, as MRD levels are generally concordant between MFC and NGS-based

techniques. Derman *et al*[68] showed a good degree of agreement between methodologies, but MS has yet to be validated as extensively as other techniques have[58, 69, 70], and the degree of comparability between LC-MS and established methods has not been determined.

6.3.1 Sequencing approaches in MM: MRD, tumor heterogeneity, and clonal evolution

In the last 15 years, the advent and decreasing cost of next-generation sequencing has allowed for the study of the genetic basis of several cancer types and complete, personalized, whole-genome sequencing. NGS of PCR-amplified, tumor-specific markers showed the potential for identifying MRD using NGS as a main instrument of detection in liquid tumors based on the ability to identify low frequency aberrant reads[71]. Because unique immunoglobulin gene rearrangements are characteristic of mature plasma cells, significant attention has been paid to next-generation sequencing of these genes and their use as biomarkers [72]. In addition, the evaluation of bulk DNA samples by NGS allows for the identification of multiple clones and subclones through the identification and frequency determination of multiple variants of a single gene[73, 74].

At present, the most widespread clinical application of NGS for MRD detection in MM targets immunoglobulin V(D)J sequences which are characteristic for clonal cells[21, 23]. These systems have been commercialized as the clonoSEQ platform (Adaptive Biotechnologies, Seattle, WA, USA), formerly known as LymphoSIGHT™ [75, 76] and LymphoTRACK™ (Invivoscribe Inc., San Diego, CA, USA) systems. clonoSEQ assay is more common and is routinely used for MRD assessment. Briefly, the procedure calls for DNA extraction from bone marrow aspirate and PCR amplification of all *IGH* loci, including the *IGH* complete and incomplete loci. The assay is based on universal PCR primers for the targeted sites, with 39 total PCR cycles and requires a minimum of 500ng gDNA input per

sample. The amplified product is then made into a library and sequenced at a median

coverage of 10x per input B cell. The assay requires an initial identification of the tumor

clonotype on diagnosis (defined as a clonotype identified as >5% of reads), and the clonotype

can then be tracked over the course of treatment[77]. LymphoTRACK, in contrast, uses

different targets within *IGH.* It is designed to be done in-house by clinical labs and can be

run on an Illumina MiSeq[69], whereas clonoSEQ is performed centrally.

A major benefit that NGS offers over other approaches is the ability to supply

qualitative data on mutation landscape, which in other cancers can indicate appropriate

courses of therapy[78, 79]. NGS does have multiple applications with respect to investigating

clonal evolution and druggable mutations, but in the context of MM MRD, the primary value

of NGS is its ability to identify very low frequency variants in a sample.

6.3.2   Circulating tumor DNA and its use in MM observation

An alternative to BMB-derived material is freely circulating cell-free DNA (cfDNA).

cfDNA is the result of normal cellular turnover as chromatin is digested by endonucleases

during apoptosis[80]. Circulating tumor DNA (ctDNA) displays good concordance with

primary tumors via whole exome sequencing (WES) in MM[45] and similar "liquid biopsies"

have been tested in active MM and other types of cancer[81-86], including a liquid biopsy for

EGFR in NSCLC which was recently FDA-approved[87].

In MM, ctDNA-based liquid biopsy has not been extensively validated in clinical

trials. Rather, a handful of trials have yielded conflicting data about the usefulness of liquid

biopsy for cfDNA. Notably, three studies analyzed V(D)J sequences in cfDNA only: Oberle

et al elected to amplify V(D)J sequences via PCR before library preparation and sequencing,

and determined only that MM-indicating V(D)J sequences are cleared from circulation more

quickly than M protein[88]; this may indicate a relationship to tumor burden, but this is disputed by conflicting results from Manier *et al*[45]. Biancon *et al*[89] took a similar approach, amplifying the *IGHJ* gene in cfDNA. They observed several clonotypes of *IGHJ* occurred in either cfDNA or isolated plasma cells, but only 11% of the clonotypes they identified occurred in both. However, they observed that all tumor-associated clonotypes were identified in both plasma cells and cfDNA. Finally, Mazzotti *et al*[90] used the clonoSEQ platform to analyze both BM samples and cfDNA. Mazzotti's group saw no correlation between MRD levels in BM and cfDNA, and saw 18 false negatives (MRD- by cfDNA analysis, MRD+ by BM analysis) out of 37 samples. However, it is unclear whether clonoSEQ is appropriate for cfDNA in MM, though it has been demonstrated in DLBCL[23].

Rustad *et al*[91] presented the first reports using ddPCR in cfDNA in MM to date (though Drandi *et al*'s original method used paired BMB and peripheral blood samples[57]), finding that this method was able to identify mutations in the MAP kinase pathway consistently, and was able to track tumor burden. However, the choice of the MAP kinase pathway as a target limits the applicability of this approach to <50%. Li *et al* were able to replicate these results, though MRD was never explicitly addressed [92].

Later, Vij *et al* used a hybrid approach, co-opting the clonoSEQ technique and using it on both cfDNA and FACS-sorted PBMCs, and comparing this approach to traditional BMB. They found good concordance between the two methods, as well as correlation between PBMC/serum clones and BMB-derived clones. Unique among these studies is that Vij *et al* also isolated RNA from PBMC and serum to search not only for the clone, but also to assess the number of clonal cells present[44].

A newer development in MM liquid biopsy is the use of low-pass whole genome sequencing (lpWGS), whereby tumor burden is calculated based on the relative magnitude of copy number aberrations in the sequenced sample. Pre-treatment application of DLBCL patients has been shown to predict risk of relapse after CAR-T therapy [93], and in MM, lpWGS helps define risk categories in multiple-refractory MM patients not receiving CAR-T[94].

6.3.3   Hybrid capture promises high sensitivity and applicability

In the context of both low disease burden, it may prove difficult to detect ctDNA and differentiate it from germline cfDNA. In addition, sheared gDNA may not be amplified appropriately if the locus of interest is not flanked by primer sites on both sides of the fragment. Both of these issues can be ameliorated through the use of hybrid capture[83, 85, 95]. Much like whole exome sequencing (WES) enrichment, hybrid capture uses oligonucleotide probes to capture specific fragments for high-throughput NGS.

Several studies have used hybrid capture to identify mutations and track disease progression in several other cancers, including breast cancer[83], lung cancer[78, 83, 96], and diffuse large B-cell lymphoma (DLBCL) [81, 86, 97] which has many parallels with MM. First published in 2014, CaPP-Seq (Cancer Personalized Profiling via Sequencing) was proposed as a method to identify somatic mutations and copy number aberrations in non-small cell lung cancer (NSCLC) patients. Newman *et al* applied an iterative algorithm to a large cohort of NSCLC tumor genomes and exomes, aiming to identify "selectors" which would find the greatest number of somatic mutations and fusion breakpoints at the shortest probe length. The group then optimized the probes on an independent NSCLC tumor cohort, and in testing patient samples, observed maximal sensitivity of 85% and maximal specificity

of 96%, with improvements as the disease progressed from stage I onwards. In addition, owing to the difficulty of biopsy in NSCLC and the confounding effects of radiotherapy on PET-CT, the authors used CaPP-Seq as a surrogate for tumor burden[96]. Working from the same lab as Newman, Scherer *et al* demonstrated high sensitivity in DLBCL and identified sequences predictive of relapse [23]. The technology is marketed under license using the Roche Avenio branding. Using a CaPP-Seq schema generalized for multiple cancers, Clark *et al* would use a similar hybrid capture design, along with unique molecular identifiers (UMI) in cfDNA and associated solid tumors, identifying disease evidence at sensitivities over 80% at a mutant allele frequency <0.25% with 100% positive predictive value, and compared favorably to established PCR methods[83].

In MM, hybrid capture-based schemes have been used to investigate cfDNA during active disease, but not to investigate MRD specifically[85, 98, 99]. Three investigations separately attempted to identify known oncogenes and *IGH* loci via hybrid capture, then use deep sequencing to identify mutants, translocations, and copy number aberrations. The studies all vary in DNA source, sample input, and targets, and among these, the target size and input are likely the most important. Common regions include member genes of the MAP kinase pathway and *IGH*. Theoretically, larger panels which target many loci would have greater sensitivity than smaller ones. However, there is an upper limit, as Manier *et al*'s WES approach only identified 20-30 genes which were useful in analysis. The sensitivity of the hybrid capture approach has not been evaluated in minimal residual disease in MM, as all of the above assays were evaluated in active disease. Though each shows high sensitivity, the ability to detect minimal residual disease using hybrid capture may depend on more than just identifying canonical mutations.

6.4 Challenges and future directions

6.4.1 Technical and comparative challenges

The ability to define and detect residual disease at sensitivity levels $>10^{-5}$ have given the myeloma community a much better understanding of the depth of response achieved by existing and novel therapies, the increasing depth of response driven by modern therapies has led to their becoming frontline strategies. Technical challenges for each approach are well-documented, but some universal challenges remain.

MFC is the gold standard in cancer treatment due to its near-universal applicability and sensitivity, but it is not without its drawbacks. All bone marrow-based assays require poorly tolerated and inefficient bone marrow biopsies (BMB)[100]. BMB are uncomfortable and invasive for patients and have a failure rate of up to 25% due to hemodilution[100]. Tumor heterogeneity is frequent in MM and a single BMB could miss some of the heterogeneity of the tumor[6]; this can be remedied somewhat via sequencing approaches or targeted biopsies (based on imaging) [45, 101], but the patchy nature of MM tumor infiltration in the medulla, as well as the presence of extramedullary disease, means that blind BM aspiration alone is an imperfect sampling strategy[102]. Finally, rapidly proliferating tumors may not be detected in the semiannual or annual intervals used for BMB and MFC analysis until they become clinically apparent, by which point the value of MRD detection is moot.

A common theme in MRD research, especially in myeloma, is that a negative result in one MRD testing modality does not necessarily predict whether a patient is truly "cured," or even whether they will test positive for MRD by another modality. The various MRD

assessment techniques have varying sensitivities, interrogate different compartments, and an

MRD- result often only indicates that the time before relapse is prolonged.

A variety of groups have attempted to measure MRD in different ways, and MRD

measurement is not standardized in methods or reporting. While ddPCR, NGS, and MFC

have all been shown to be roughly comparable[58], efforts to standardize MRD reporting

have only come to fruition in the last few years[102], so older studies must be compared in

light of their differences in design and methodology.

Sensitivity of both MFC and NGS have increased to the point that sensitivity is

ultimately bound by sample input: for example, an input of 10^6 cells into NGF analysis can

reasonably be expected to have a sensitivity of 10^{-6}, and the same is roughly true (though not

entirely) for NGS-based approaches[103]. Though the sensitivity of NGS approaches is

comparable to, or surpassing, that of NGF, increased sensitivity comes with its own technical

challenges, not least of which the necessary input material to achieve greater sensitivity: due

to the statistical "rule of three," to achieve a 10^{-7} sensitivity using NGF, $3x10^7$ bone marrow

cells would be necessary[104, 105]. For a complex NGS assay involving hybrid capture and

NGS, library preparation and multiplexing each require subsampling steps. Assuming

sufficient read depth, the probability of detecting target molecules in a healthy background is

determined by Poisson probability distributions, and this probability decreases based on the

number of subsampling steps[106]. NGS approaches are also limited by PCR-induced bias

and the error rate of the sequencing platform used. Finally, a common practice in NGS-based

approaches is sample multiplexing, which can produce cross-contamination and index

hopping, leading to false positives[107]. While multiplexing, subsampling, and unnecessary

PCR cycles could be avoided or mitigated, this has the potential to make each assay

extravagantly expensive. Some researchers have suggested that NGS assays be performed in triplicate, further adding to the cost of these techniques[56]. Pushing to 10^{-7} or deeper may not be possible with current technology or even particularly informative unless that level of response can be shown to have a survival advantage over detection at 10^{-6}, the current limit. While increasing sensitivity of MRD assays may be worthwhile, a more important challenge may simply be to have a greater proportion of patients achieve sustained MRD negativity after therapy. In this light, MRD outcome may be highly useful as a secondary endpoint for clinical trials in MM.

6.4.2 Minimizing sequencing error

Error is inevitable when using NGS, and although modern sequencers have improved error rates compared to previous generations, error rates on the order of 1×10^{-4} bases read are standard when sequencing at great depth [108]. Furthermore, PCR misincorporation errors can occur at rates ranging from 1.5×10^{-4} (*Taq*) to 5.3×10^{-7} (high-fidelity Q5 polymerase)[109]. To mitigate sources of sequencing and polymerase errors, multiple error suppression methods have been proposed.

Molecular barcoding, first proposed by Miner *et al* [110], is the process of introducing a degenerate nucleotide tag sequence to each input DNA molecule during library construction, which allows sequenced molecules to be identified as authentic sequences, duplicates (thus allowing quantitation of duplicates), and further allows the identification of errors within individual molecules [111, 112]. Use of these nucleotide barcodes, or unique molecular identifiers (UMIs) allowed improvement of error detection by requiring the identification of "super-mutants," mutants present on ≥95% of reads of a single molecule family. This approach improved the accuracy of NGS-based analysis of very low-frequency

16

mutation rates in human germline DNA and other sources, showing substantial decreases in variant allele frequencies identified by these modalities[112].

Duplex sequencing, an extension of these ideas, incorporates dual UMIs, one unique tag on each end of the insert molecule, and requires *in silico* matching of the sequenced strands into read families to confirm the authenticity of variants present on both strands, as opposed to polymerase errors introduced at any point, even the initial amplification step. Drawing on earlier approaches, this method generates a single strand consensus sequence (SSCS) from each strand of the original molecule, and then reconciles the SSCS from both strand families into a dual strand consensus sequence (DSCS) for the insert molecule. As such, variants only recognized on the read family for one strand can be classified as polymerase errors, as are any variants identified in any smaller portion of the reads for one strand[113]. One drawback of Duplex sequencing, however, is that reconciling SSCS to DSCS is difficult, and the majority of reads are not able to be reconciled into DSCS. As a result, it is impractical and uneconomical to sequence samples to a duplex depth (depth of a locus covered by DSCS-reconciled reads) to an equivalent SSCS depth[114].

Additional efforts to improve sequencing accuracy include *in silico* error suppression methods, predicated on the fact that sequencing errors are stereotypic, and the predominant class of errors (G→T transversions, C→T and G→A transitions) are the result of oxidative damage during enzymatic and hybridization reactions. Furthermore, the possibility of a given base being a false mutation can be judged against the probability of finding a similar mutation in the same locus in a panel of healthy controls, allowing greater confidence in true variant calls when a panel of normal samples is included in the analysis[115]. Another novel

17

strategy to detect variants accurately at low frequencies is to specifically look for phased mutants, i.e. two specific variants in short succession on a molecule[116]

6.5 Utilizing highly sensitive methods of assessing disease burden for prognostication of disease course

While the correlation between various genetic factors and disease outcome has been understood for decades, and while sequencing studies in the past fifteen years have elucidated the effects of specific mutations, using these data in real-time to observe and potentially predict therapy response is a fledgling field. The relative invasiveness of the main MRD detection methods suggest that assays relying on the bone marrow compartment are not ideal for providing useful data in dynamic treatment settings. However, many schema relying on peripheral blood have demonstrated prognostic ability, both in MM and in other B cell malignancies.

This discussion is particularly relevant in the context of chimeric antigen receptor T cell therapy (CAR-T), which has a unique response profile. As described above, CAR-T therapy causes durable responses in roughly half of patients, while the other half experience disease progression within months of infusion. Combined with the significant turnaround time of six weeks to manufacture autologous CAR-T cells and the significant expenses involved in the therapy, the ability to predict which patients would respond well to CAR-T therapy could guide treatment decisions, thereby preventing a waste of time and resources. On the other hand, the novel nature of CAR-T treatment, combined with extensive inpatient time surrounding treatment, makes CAR-T therapy an excellent subject for comprehensive and rigorous study.

Analysis of sFLC and immunofixation of immunoglobulins surrounding CAR-T therapy indicates that the change from baseline M protein level presents as a rapid decline over the first month before plateauing and eventually rising if the patient relapses, consistent with responses of this biomarker to traditional therapy [117]. In addition, outside the CAR-T context, Manier *et al* [45] show that disease burden assessed by cfDNA low-pass WGS correlates with M protein levels and disease burden. Data demonstrating the utility of the LC-MS approach described earlier in the context of CAR-T therapy are not available, but could provide a promising avenue to utilize liquid biopsies in dynamic treatment settings.

In the context of diffuse large B cell lymphoma, our group has shown the ability of CaPP-Seq to discriminate patients into "responders" and "nonresponders" on the basis of a five-fold decrease in variant allele frequency in ctDNA within seven days post-infusion of anti-CD19 Axicabtagene ciloleucel (Axi-cel)[118]. To our knowledge, this study is unique in that it investigates disease burden in a very short duration after transfusion, whereas the majority of studies of CAR-T therapy for lymphoid malignancies do not examine disease responses for at least one month after infusion, when response and MRD status are evaluated. However, given that ide-cel CAR-T cells expand to their maximum number during the first week of therapy before slowly declining over several months[15], it is possible that tumor burden may regress within the first week of therapy[Martinez], consistent with Deng *et al*'s study of DLBCL.

7   **Justification, hypotheses, and aims**

Chimeric antigen receptor T cell therapy is a novel adoptive cell therapy which shows considerable promise in multiple myeloma and leads to rapid shrinking of the tumor within one month of infusion[14]. CAR-T numbers peak within one week of infusion[15], but the most sensitive methods of detecting residual tumor cells (Minimal Residual Disease, MRD), methods which are prognostic in nature[13, 17, 18]. are not able to monitor disease burden in such a dynamic timeframe owing to their reliance on poorly-tolerated bone marrow biopsies. An attractive alternative to bone marrow biopsies presents itself in cell-free DNA (cfDNA) which is shed into the bloodstream by apoptotic cells throughout the body. Circulating tumor DNA (ctDNA) displays good concordance with whole exome sequencing (WES) in MM[45] and similar "liquid biopsies" have been tested in active MM and other types of cancer[81-87]. A unique challenge of detecting low disease burden in cfDNA is the expected low copy number of ctDNA, but this may be ameliorated through the use of hybrid capture[83, 85, 95], which uses oligonucleotide probes to capture specific fragments for enrichment before high-throughput NGS. We have designed a custom hybrid capture probe panel and intend to apply it to serial cfDNA samples of patients receiving CAR-T therapy in order to test results demonstrated by Deng et al[118], who showed that a fivefold decrease in variant allele frequency, as determined by ctDNA capture sequencing, within seven days of CAR-T infusion was predictive of treatment response in diffuse large B cell lymphoma (DLBCL). The central hypothesis is that our approach, using cfDNA, hybrid capture, and deep sequencing, which we refer to as M5Seq (myeloma molecular residual disease monitoring by massively parallel mutation sequencing), will have sensitivity equivalent to or exceeding

standard of care MRD measurement techniques. Furthermore, we hypothesize that the sequencing data which results will be useful for predicting outcomes.

The specific aims of this project are:

7.1 Aim 1: Determine the limit of detection and limit of linearity of the M5Seq assay

Next generation sequencing, using advanced digital error suppression and molecular barcodes, is able to identify and quantitate ultra-low frequency variants in genomic and cell-free DNA, including the identification of ultra-low frequency tumor-derived variants when using custom hybrid capture panels[96], at allele frequencies of 0.01% and lower. Similarly, standard of care MRD assays frequently achieve this level of sensitivity [29, 75]. I hypothesize that M5Seq will be able to detect variants with similar sensitivity to existing methods, and that it will retain linearity down to its limit of analytical sensitivity. In order to demonstrate the limit of sensitivity of M5Seq, spike-in libraries consisting of serial dilutions of tumor-derived DNA in healthy DNA will be captured and sequenced, and the variant allele frequency for individual variants will be plotted down the dilution series to a lower limit of 10-6. To eliminate the influence of confounding variants, a panel of healthy cfDNA controls will be captured and sequenced, and variants identified in more than 1 normal sample will be filtered. In addition, population-level variants identified in the ExAC browser above a population allele fraction of 1% will be filtered.

7.2 Aim 2: Investigate the informative and prognostic abilities of M5Seq in patients receiving standard of care treatment.

Exome sequencing demonstrates strong concordance between cfDNA and tumor gDNA in lymphoid malignancies[23, 86, 96] including MM[45]. Furthermore, ctDNA

sequencing is predictive of outcomes in DLBCL, including in the days following CAR-T therapy[23, 97, 118]. I hypothesize that when utilizing M5Seq, variants called in bone marrow and contemporaneous samples will demonstrate good concordance. I further hypothesize that change in VAF within two to seven days after CAR-T infusion will be predictive of outcomes. First, we intend to sequence matched, contemporaneous pre-treatment cfDNA and bone marrow samples taken from treatment-naïve MM patients to demonstrate inter-compartment concordance and applicability of ctDNA sequencing as an indirect indicator of tumor burden. Second, we intend to evaluate changes in VAF over the seven days after CAR-T infusion and determine whether these changes are correlative with IMWG-defined response at D+30 or survival.

The successful accomplishment of Aim 1 will allow for accurate quantitation of low-frequency, tumor-derived variants and establish the analytical sensitivity of the assay when compared to MRD assays. The successful accomplishment of Aim 2 will demonstrate the clinical and prognostic abilities of M5Seq, providing better information to clinicians and scientists as CAR-T therapy in MM evolves.

8   Methodology

Isolate cfDNA/prepare spike-ins

Quality control

Hybrid capture

SarahKusula 2012, Wikimedia

Preparation duplex-UMI NGS library

Sequence

Analyze

CGAATGCG
GTCGTGAC
TAACGTGG

Figure 1: Schematic of methodology employed

The sample processing workflow for all samples consisted of six discrete steps (fig.1, from top left following arrows). DNA was extracted from patient plasma and primary tumor samples, and the extracted DNA was assessed for quality in order to determine which timepoints to assess, when possible. Sequencing libraries were constructed from these DNA samples, and the libraries were enriched using hybrid capture. Captured libraries were sequenced and the resulting data were analyzed using a publicly available bioinformatics process.

8.1   Sample acquisition and sources

Clinical samples were acquired from two different sources: first, a standard-of-care clinical specimen collection protocol (PA19-0436) for newly-diagnosed MM patients ("NDMM cohort") receiving bortezomib, lenalidomide, and dexamethasone therapy (VRd) and an autologous stem cell transplant. Of these, 11 patients were identified as being candidates for analysis due to the presence of multiple induction samples and post-transplant samples, and of these, one bone marrow-derived library failed QC. Second, relapsed/refractory MM (RRMM) patients receiving ABECMA (idecabtagene vicleucel, Bristol Myers Squibb, referred to herein as "ABECMA protocol" or "ABECMA cohort") anti-B Cell Maturation Antigen CAR-T therapy (n=19).

8.2   Spike-in experiments

Genomic DNA (gDNA) from peripheral mononuclear blood cells (PBMC, from MD Anderson Cancer Center blood bank) and cell lines U266 and H929 (American Type Culture Collection) was extracted using the Qiagen Blood Spin mini Kit according to manufacturer's

protocol and quantified using Qubit 3.0 fluorometry (ThermoFisher Scientific). DNA was

sonicated to 150bp using a Covaris M platform, and the sonicated product was diluted to

50ng/μL. The following samples were prepared for library prep, using 1/10 serial dilutions

(see table 1 for DNA input and expected allele fractions). Positive controls contained only

cell line (U266 or H929) DNA, processed as described; negative controls contained only

PBMC DNA, again processed as described. Each library had an input of 1500ng of DNA, as

quantified before shearing per manufacturer directions, and suspended in 30μL of ultrapure

water.

Table 1: Experimental design of spike-ins

Variant Allele Freq.	log10	Cell Line DNA (ng)	PBMC DNA (ng)
1 (Positive Control)	0	1500	0
0.1	-1	150	1350
0.01	-2	15	1485
0.001	-3	1.5	1498.5
0.0001	-4	0.15	1499.85
0.00001	-5	0.0015	1499.985
0.000001	-6	0.00015	1499.9985
0 (Negative Control)	NA	0	1500

8.3   Nucleic acid extraction

In accordance with the MD Anderson Cancer Center clinical specimen protocol

PA19-0436, 10mL blood samples were collected from patients at diagnosis of MM and twice

centrifuged to obtain plasma.

10mL blood samples were collected from patients receiving ide-cel on the following

schedule. Samples were twice centrifuged to obtain plasma.

- At apheresis for CAR-T manufacture

- Days -5, 0, +1, +4, +7, +14, +21 +28 from CAR-T infusion (±2 days for each timepoint before 14 days, then ±3 days for subsequent timepoints)

- Every 30 days after infusion until discontinuation or withdrawal, up to 120 days

In addition, 16 banked plasma samples from the MD Anderson Cancer Center blood bank were thawed and aliquoted into 15mL tubes. All researchers were blind to the identity or clinical characteristics of the normal samples, which contributed to the Panel of Normals (PoN).

cfDNA was extracted from plasma using the QIAGEN Circulating Nucleic Acid kit (QIAGEN, Hilden, DE) according to manufacturer's protocol and eluted in 35μL PCR-grade water. Eluent was then quantitated using the Qubit 3.0 and Qubit High Sensitivity reagents, and analyzed using Agilent Tapestation D1000 to assess quality and purity of cfDNA.

Bone marrow samples were processed by the MD Anderson Cancer Center Lymphoma Tissue Bank and viably cryopreserved. These samples, containing over one million cells each, were spun down and washed twice in phosphate-buffered saline before resuspension in Qiagen RLT Plus buffer. Bulk nucleic acids were extracted using the Qiagen Allprep kit. DNA was quantitated using the Qubit 3.0 with Qubit High Sensitivity reagents before shearing using the Covaris M platform.

8.4   Library construction, hybrid capture, and sequencing

The samples then underwent library construction using Twinstrand library and capture kits (Twinstrand Biosciences, Seattle, WA), using dual index universal molecular identifier stubby indexing adapters (UDI). All library preparation was carried out in 96 well plates to limit variability. End repair and A-tailing was performed in a thermocycler (20°C

for 30min, then 65°C for 30 minutes), followed by UDI adapter ligation for one hour at 20°C in a thermocycler. The ligated product was bound to a 0.8x suspension of SPRI beads and cleaned using 70% ethanol to remove adapter dimers and enzymes from the ligation reaction before resuspension in low-TE buffer. The product was conditioned using Twinstrand Library Conditioning Mix by incubation at 37°C for one hour. The product was then amplified using PCR (10 cycles) and cleaned with a 1.0x ratio of SPRI beads. Final libraries were analyzed via Agilent Tapestation to check for quality, fragment size, and purity. 1µL of library was diluted 1/10 and used for QC, then stored for low-passage whole genome sequencing (lpWGS).

The first of two overnight hybridization reactions was conducted using a custom probe set at 65°C. The hybridization mixture incubated for no less than 14 hours (and up to 20) with biotinylated probes before being transferred onto washed streptavidin beads and incubating for another 45 minutes to capture hybridized molecules on the beads. Washes occurred at room temperature, following manufacturer protocols. Captured libraries were amplified by PCR (16 cycles) and cleaned with a 1.0x ratio of SPRI beads before quantitation and QC.

The second overnight hybridization proceeded the same as the first hybridization, except that the incubation temperature was 62°C, again in keeping with manufacturer protocol. Captured libraries were amplified using PCR (6 cycles) and cleaned with a 1.0x ratio of SPRI beads before final quantitation and QC. Captured libraries were stored in low-TE buffer in 96 well plates at -20°C.

Following manufacturer recommendation for achieving maximum mean duplex depth, samples were sequenced according to the following scheme:

$$\text{\# Paired End Reads} = 1.08 \times 10^6 \text{ x DNA input (ng) x Conversion Factor}$$

Such that 1.08×10^6 is a panel-specific requirement, and the conversion factor is an integer n=1 for sheared gDNA and n=3 for cell-free DNA. So, for example, bone marrow samples with 250ng input would call for:

$$\text{\# PE reads} = 1.08 \times 10^6 \text{ x 250ng x 1} = 270 \text{ million reads}$$

And a cfDNA sample with 50ng input would require:

$$\text{\# PE reads} = 1.08 \times 10^6 \text{ x 50ng x 3} = 162 \text{ million reads}$$

Samples were pooled proportional to the number of reads required and sequenced on S4 lanes on an Illumina NovaSeq system, using paired-end 100bp reads.

8.5   Capture panel design

An initial capture panel design was created using hg19 according to the method described by Newman[96] based on MM exomes publicly available in the Multiple Myeloma Research Foundation CoMMpass database (Green lab, unpublished data). This panel, MM_M4, was then significantly redesigned and modified. First, MM_M4 was lifted over using the UCSC Genome Browser to hg38. Each existing probe was analyzed for secondary structure and number of BLAST hits. Probes with $\Delta G° > -15$ for RNA folding, and probes with >5 BLAST hits, length of >70bp, and >80% similarity were eligible for removal from the panel. Genes in these categories typically consisted of somatic hypermutation targets and *Ig* genes, respectively.

At this point, the decision was made to salvage these regions when possible, as the mutational signature of MM does include several SHM targets and a clonotypic peptide sequence. Regions to be probed were identified by selecting the 500 most-commonly mutated genes and noncoding regions in the MM genome [119]. The exon start and stop

locations in hg38 were pulled for each region and compiled. These short regions were tiled

and QC'd as described in the previous paragraph. Preference for salvage was given to known

oncogenes such as *BRAF, KRAS, NRAS,* and *MYD88*. The final panel, manufactured as

pan00309 (M5Seq) was manufactured by Twinstrand Biosciences and covered 186kb.

8.6   Sequence data analysis and VFC calculation

The bioinformatics analysis used for this process is the CAPP_SEQ_pipeline,

publicly available on GitHub (https://github.com/Green-Lab-

MDACC/CAPP_SEQ_pipeline). FASTQ R1 and R2 read files were checked for quality

using FastQC (https://www.bioinformatics.babraham.ac.uk/projects/fastqc/), and then

converted to unaligned BAM files using the fgbio FastqToBam package

(http://fulcrumgenomics.github.io/fgbio/). UMIs were extracted using the fgbio

ExtractUmisFromBam package, and the reads were then converted to interleaved FASTQ

files using the Picard SamToFastq (https://github.com/broadinstitute/picard) and aligned to

the hg38 genome using BWA (http://bio-bwa.sourceforge.net/bwa.shtml) and Picard

MergeBamAlignment packages. Reads were then grouped by UMI using fgbio

GroupReadsByUmi and, depending on whether duplex consensus reads were required or not,

were called using fgbio CallDuplexConsensusReads or CallMolecularConsensusReads (for

single strand consensus), with a minimum of 2 matched reads to be called. The data were

then again converted to interleaved FASTQ as described above. Reads were filtered for

quality and consensus using fgbio FilterConsensusReads and clipped using fgbio ClipBam.

Variants were called using GATK HaplotypeCaller and Mutect2

(https://gatk.broadinstitute.org/hc/en-us). Final reads were enumerated using bcftools, and

data were filtered such that only variants with depth greater than 100 were considered for

further analysis. In addition, variants previously identified in the Panel of Normals (previously called using DSCS) are filtered at this stage. At this stage, variant allele frequency (VAF) is quantitated for every called variant.

The Panel of Normals (PoN, n=15) were processed first and variants were called irrespective of variant allele frequency (VAF) or known population allele frequency (PAF), using DSCS. All variants present in more than one member of the cohort (equivalent PAF = 6.67%) were filtered from subsequent samples. In addition, all called variants are annotated with PAF as listed in the ExAC database[120] by SeattleSeq[121] and any called variants with PAF >1% are filtered from further analysis. SeattleSeq also annotated SNPs in the dbSNP database[122] and variants identified as being repeats using the repeatMasker function; these annotated variants were also filtered from analysis.

Spike-in series were screened as described above. Variants were called using DSCS in the U266+ and H929+ samples and using SSCS for all subsequent samples. The VAF of filtered variants identified in the positive control (U266+ and H929+, see Table 1) and not in U266- were plotted against the expected allele fraction (EAF), the dividend of the observed VAF (oVAF) in U266+ and the dilution factor.

Calibration timepoint samples (i.e. samples taken contemporaneously before therapy intervention, either via VRd or pre-CAR-T lymphodepletion) were processed using both the DSCS pipeline in order to call variants with low probability of being sequencing or polymerase errors, and using the SSCS pipeline for comparison. Longitudinal samples, however, are processed on the SSCS pipeline, with special attention paid to the variants defined by the calibration sample's DCSC data.

After filtering, final sequencing data were processed in Excel, including Variant Allele Frequency Fold Change (VFC), the quotient of the average filtered VAF at a given timepoint over the D+0 average filtered VAF. Survival analysis was performed, and hazard ratios were calculated, in Graphpad Prism 9. Graphics were generated using Python's Plotly package, Graphpad Prism 9, or Excel. Statistical analyses were performed in Graphpad Prism 9.

9   Results

9.1   M5Seq panel validation *in-silico*

The redesigned capture panel was tested *in silico* to assess the applicability of the M5Seq panel to the initial 1,212-tumor design and validation cohorts used to design the MM_M4 panel. Called variants from each tumor which were located in the regions mapped by the probes were counted as detected variants.

Of the 1,212 tumors, 1,173 tumors contained mutations covered by the M5Seq panel (96.8% applicability rate). 315/1,212 tumors had 1-5 mutations covered (26.0%), 383/1,212 tumors had 6-10 mutations covered (31.6%), 399/1,212 tumors had 11-25 mutations covered (32.9%), and 76/1,212 tumors had >25 mutations covered (6.3%)(fig.2b). The greatest number of mutations identified in one tumor was 317. The mode of the data was 6 mutations covered per tumor, and the median was 9 mutations covered per tumor (fig.2a).
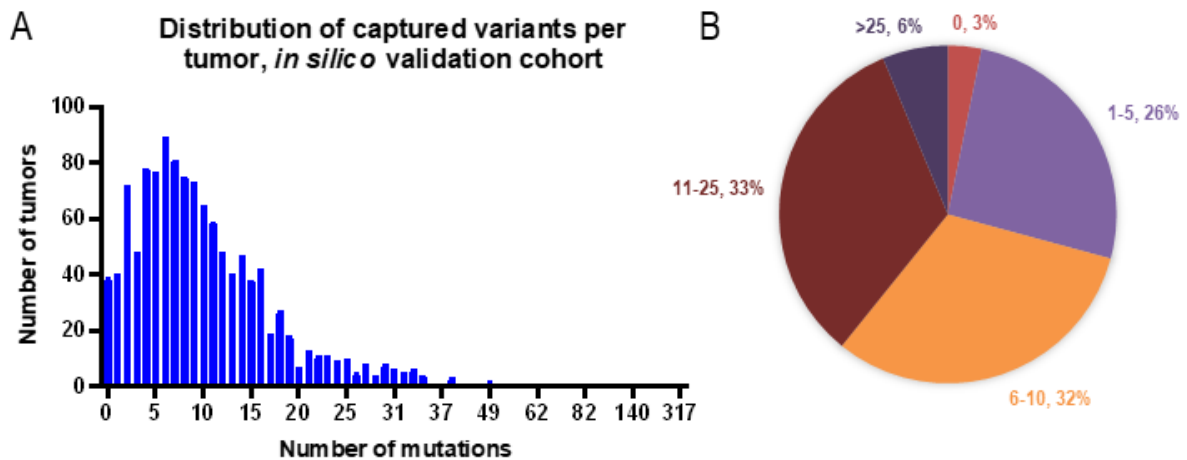
Figure 2: Distribution of mutations directed by M5Seq in silico A) Distribution of captured variants in testing and validation cohorts of the M5Seq panel. B) Percentage of tumors in testing and validation cohorts with a given range of mutations captured by M5Seq.

9.2   Analytical sensitivity of M5Seq assay
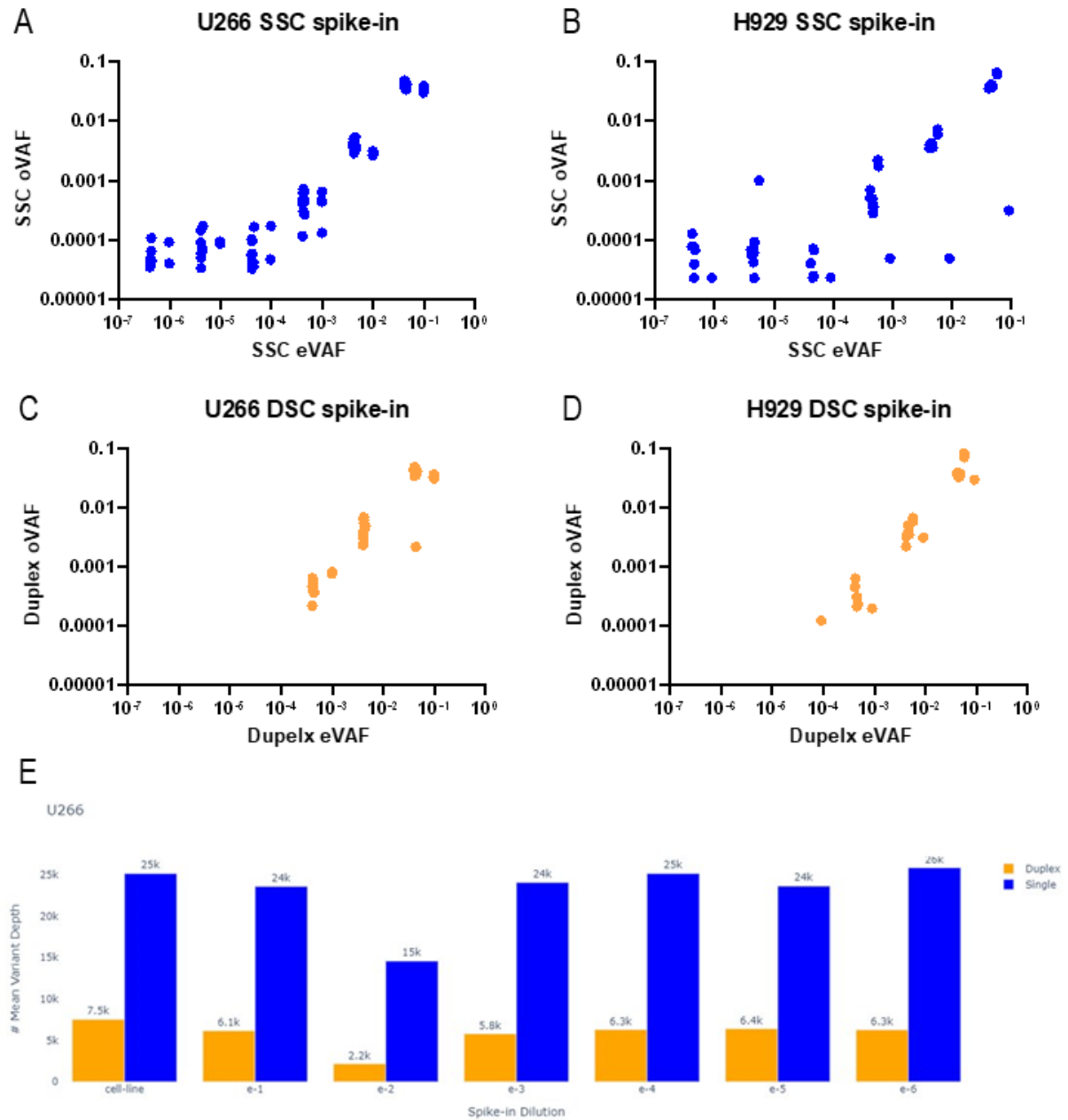
Figure 3: Results of spike-in experiments A) observed vs expected variant allele frequencies (oVAF vs eVAF) for spike-in experiments using the U266 cell line and counting single strand-supported variants which were originally confirmed via duplex sequencing in the calibration sample. B) oVAF vs eVAF for spike-in experiments using the H929 cell line and counting single strand-supported variants which were originally confirmed via duplex sequencing in the calibration sample. C) oVAF vs eVAF for spike-in experiments using the U266 cell line and only using duplex sequencing for all libraries. D) oVAF vs eVAF for spike-in experiments using the H929 cell line and only using duplex sequencing for all

libraries. E) Comparison of sequencing depth in U266 spike-in libraries when using single strand consensus sequencing vs duplex consensus sequencing.

Spike-in experiments were conducted using the U266 and H929 cell lines. Observed allele fraction (oVAF) were plotted against expected allele fraction (EAF), as calculated using the method in the Methods section. Briefly, for each variant in the U266+ library which was not filtered out, the VAF of the variant was calculated by dividing the number of variant reads by the number of total reads at the locus (oVAF). The oVAF in the U266+ library was then divided by the dilution factor to compute EAF for each variant. This was plotted against the oVAF for the corresponding variant.

When using DSCS support, the U266 spike-in series demonstrated a limit of sensitivity at 2×10^{-4} and remained linear on a logarithmic scale down the dilution series to an EAF of 2×10^{-4} (fig.3c) When using SSCS support, the U266 spike-in series demonstrated a limit of sensitivity at 3×10^{-5} and a limit of linearity at an EAF of 10^{-4} (fig.3a)

When using DSCS support, the H929 spike-in series demonstrated a limit of sensitivity of 10^{-4} and remained linear on a logarithmic scale down the dilution series to an EAF of 10^{-4} (fig.3d) When using SSCS support, the H929 spike-in series demonstrated a limit of sensitivity of 3×10^{-5} and a limit of linearity at an EAF of 10^{-4} (fig.3b).

9.3 Newly Diagnosed Multiple Myeloma (NDMM) cohort

9.3.1 NDMM patients, samples, and calibration timepoints

11 newly diagnosed MM patients, having all three of a calibration bone marrow sample, contemporaneous plasma sample, and longitudinal plasma samples for response assessment were considered for analysis here. Patients began physician-ordered frontline therapy after collection of samples. Of the 11 patients, one (MM0008) had their calibration bone marrow library fail sequencing QC. A total of 10 patients are analyzed here.
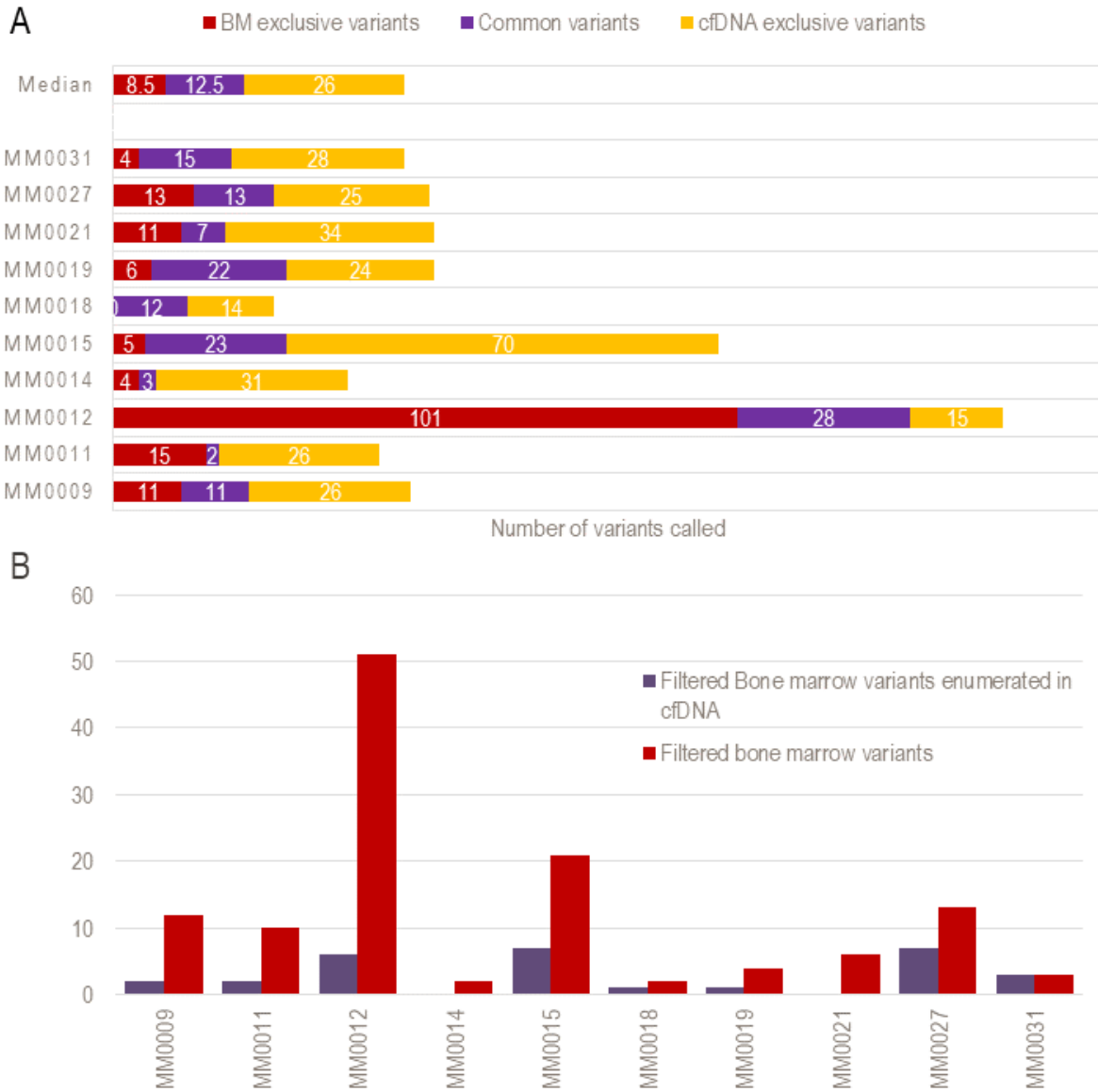
Figure 4: Inter-compartment concordance in NDMM cohort A) Number of duplex consensus variants called in bone marrow, cfDNA, and in both compartments in the NDMM cohort. B) Number of bone marrow variants clearing stringent filters for germline variants and number of these variants enumerated in cfDNA.

Comparison of pre-treatment variants called in DSCS between bone marrow and

cfDNA compartments in this cohort indicates a median of 4 variants called in bone marrow

(range 1-10) and a median of 9 variants called in cfDNA (range 4-39). The median number of concordant variants was 2 (range 0-9). The median concordance, or percentage of variants identified in both compartments, was 21% (range 0%-90%). Of the 10 patients, MM0015 had the greatest mutational burden with 39 total variants identified, whereas MM0018 had the lowest mutational burden with only 5 total variants identified (fig.4a)

Comparison of SSCS-called variants in cfDNA to DSCS-calibrated BM variants indicates that a minority of the BM-calibrated variants are recovered in cfDNA. While all three filtered, calibrated bone marrow variants were recovered in the cfDNA of patient MM0031, none of the two bone marrow variants were recovered for MM0014. For patient MM0012, despite having 51 filtered variants calibrated, only six were recovered in cfDNA (fig.4b).

Variants identified in the calibration timepoints consisted predominantly of somatic hypermutation targets such as *BTG2, BCL6, BCL2,* and *DTX1,* of which multiple variants per gene were detected in every pre-treatment PA19 sample. Other frequent SHM variants identified were *CXCR4,* and *PAX5.* At least one variant in the *IRF4* oncogene was identified all but one sample (MM0021_001, a bone marrow sample), but other oncogenes were detected at much lower rates: *TRAF3* variants were detected in a majority of patients, while *IRF8* and *TP53* variants were only detected in a minority, and a *BRAF* variant was identified in a single sample, the cfDNA sample MM0019_002, and not confirmed in the matching bone marrow sample MM0019_001 (fig.5a). The panel did not detect variants of known MM oncogenes *NRAS, FAM46C,* or *DIS3.*
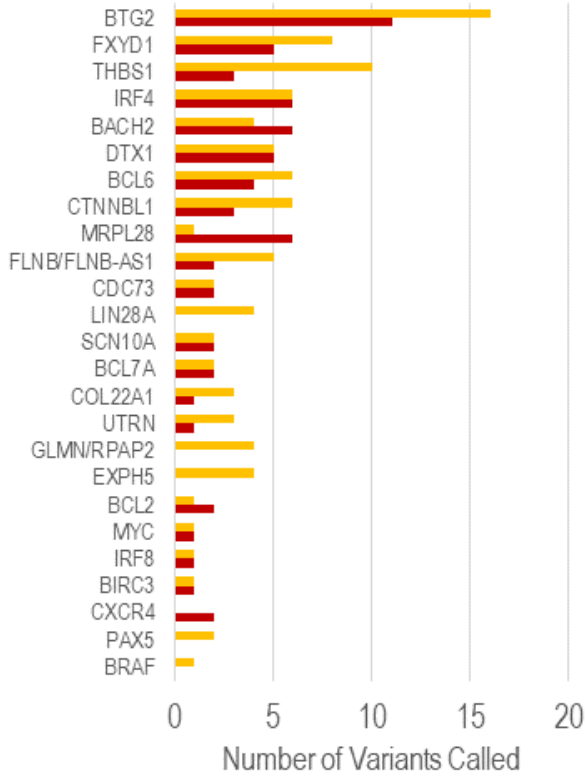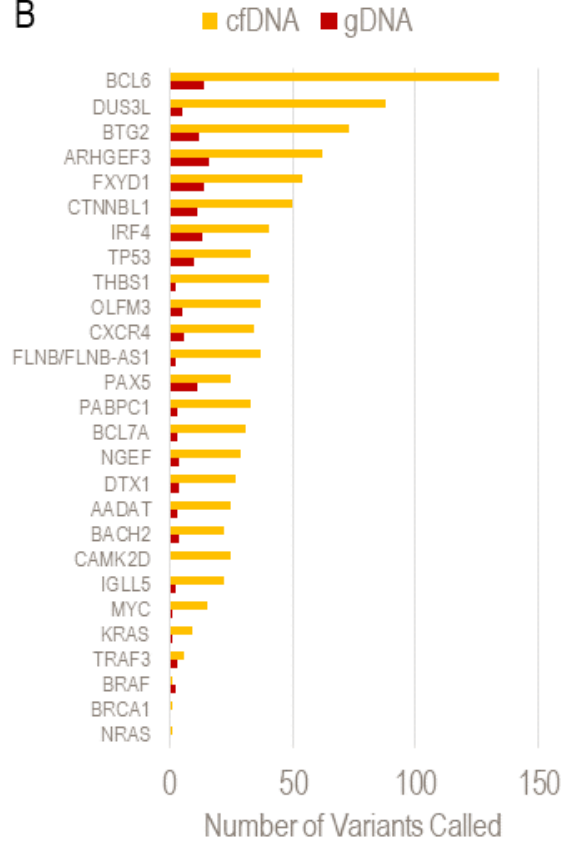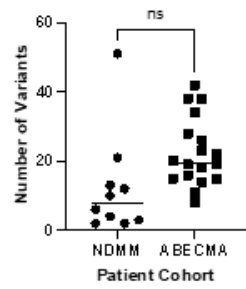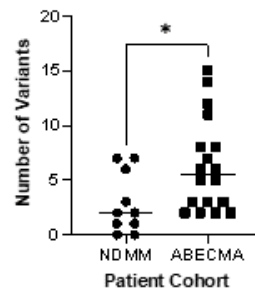
37
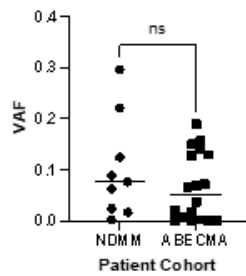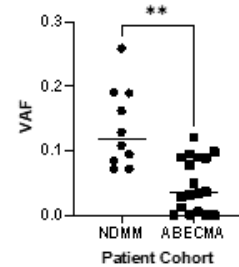
Figure 5: Comparison of calibration timepoints of NDMM and ABECMA cohorts A) Frequency of variants identified for selected genes in the NDMM cohort. B) Frequency of variants identified for selected genes in the ABECMA cohort. C) Comparison of variants identified in bone marrow of both cohorts. D) Comparison of the number of stringently filtered variants enumerated in cfDNA at calibration from both cohorts. E) Average VAF, measured using duplex consensus sequencing, at the calibration timepoint in both cohorts. F) Average VAF of enumerated variants in cfDNA at the calibration timepoint.

9.4 ABECMA

9.4.1 ABECMA patients, samples, and overall outcomes

Also included in analysis were 19 patients receiving idecabtagene vicleucel anti-BCMA chimeric antigen receptor T cell therapy. These patients were enrolled in a separate clinical trial (table 2).

Table 2: Characteristics of ABECMA cohort

Sex, % (n)	37% Female (7) 63% Male (12)
Notable previous therapies	BCMA therapy: 21% (4) IL-15: 5% (1)
Day 30 IMWG Response (Progressive Disease (PD), Stable Disease/Marginal Response (SD/MR), Partial Response (PR), Very Good Partial Response (VGPR), Complete Response (CR), Stringent Complete Response (sCR)	Deceased: 1 PD: 1 SD/MR: 4 PR: 1 VGPR: 2 CR: 1 sCR: 6 No infusion: 3
Day 30 MRD Status (EuroFlow method)	Positive: 4 Negative: 10 Deceased:1 No infusion: 3 Unknown: 1
3 Month Response	PD: 0 SD/MR: 0 PR: 1 VGPR: 1 CR: 0 sCR: 5 Deceased:7 Unknown: 5
3 Month MRD Status	Positive: 1 Negative: 2 Deceased: 7 Unknown: 9

Of the 19 evaluable patients, 11 died as of 27Apr2022, including two (AB14 and AB16) who died before receiving their infusions; as such, their pre-treatment samples are included in analysis of inter-sample concordance, but longitudinal analysis is not possible. The causes of death, when reported, were myeloma and/or related complications (3), cytokine release syndrome (1), and COVID-19-related acute respiratory distress syndrome (1). The median survival after infusion was 195 days. One patient, AB17, received an infusion but did not provide a calibration BM sample; this patient is not one of the 19 analyzed. Four patients received previous anti-BCMA therapy before receiving CAR-T infusion. Of the four, two have died. Of the two, one death was attributed to COVID-19 ARDS, while the other cause of death was unreported.

The clinical courses of two patients, AB11 and AB13, are notable. AB11 received their CAR-T infusion and experienced grade 5 cytokine release syndrome (CRS), hemophagocytic lymphohistiocytosis (HLH), and a systemic bacterial infection. The final sample from AB11 was collected on D+7 and was captured and sequenced. AB11 died on D+14 due to complications; MM was not listed as a cause of death. Due to the unique clinical outcome, and also owing to the abnormally high cfDNA yields from her plasma samples, the patient will be analyzed separately when appropriate. Patient AB13 received their infusion and was diagnosed with stable disease per IMWG criteria at her one-month follow-up. AB13 died of COVID-19-related acute respiratory distress syndrome 42 days after infusion; as such, this patient will be censored from survival analysis as well; however, the change in VAF over time is still useful with respect to their D+30 response.

9.4.2   Inter-compartment concordance of variants identified in ABECMA samples

41
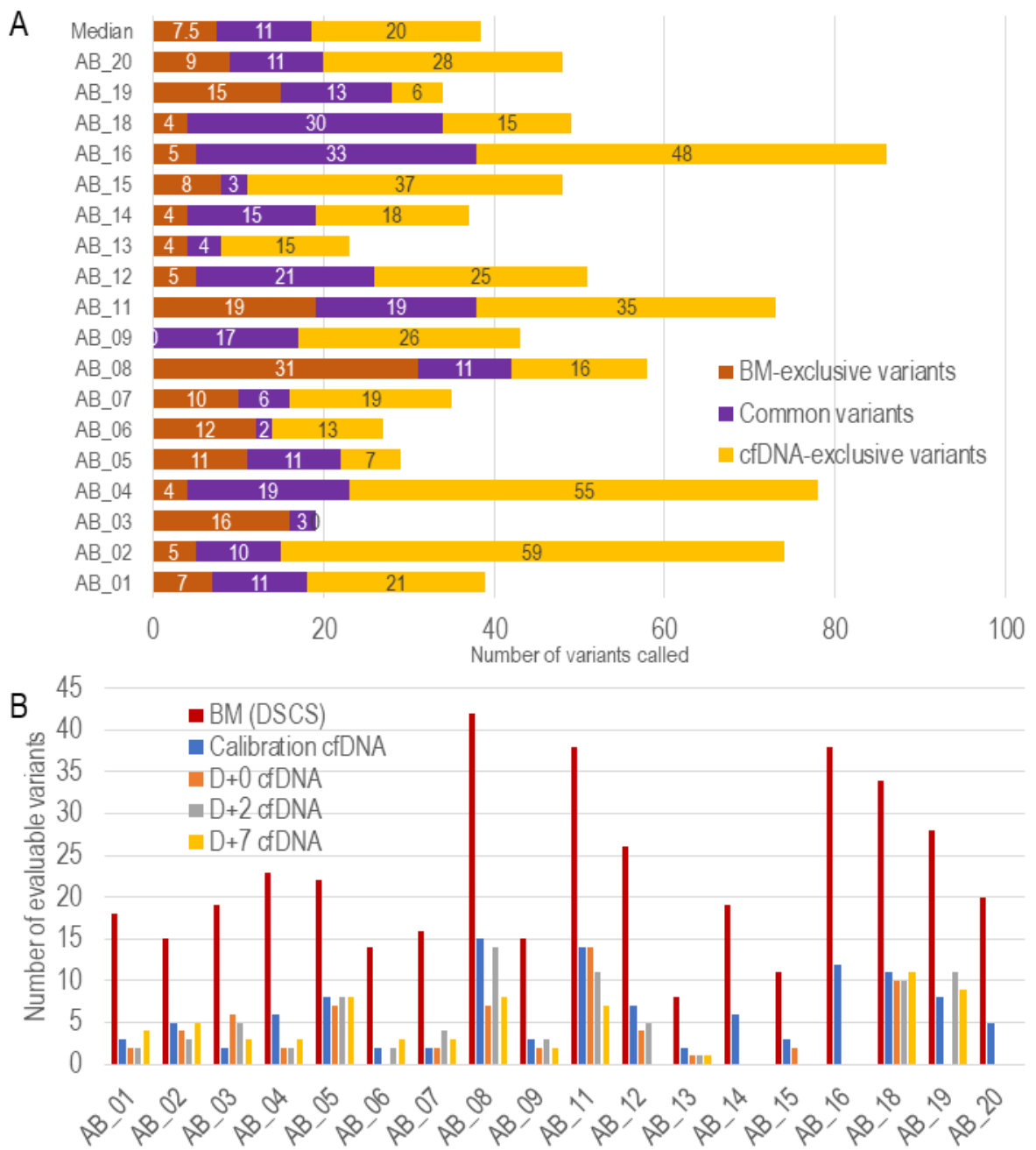
Figure 6: Inter-compartment concordance in ABECMA cohort A) Number of duplex consensus variants called in bone marrow, cfDNA, and in both compartments in the NDMM cohort. B) Number of bone marrow variants clearing stringent filters for germline variants and number of these variants enumerated in cfDNA at multiple timepoints, including at calibration (contemporaneous with bone marrow aspiration), D+0, +2, and +7 of CAR-T infusion.

Comparison of pre-treatment variants called in DSCS between bone marrow and cfDNA compartments in this cohort indicates a median of 19.5 variants (range 8-42) called in bone marrow and 36 variants (range 3-81) called in cfDNA, of which a median 11 variants (range 2-31) were identified in both compartments. The median concordance, or the percentage of variants identified in both compartments from the total number of variants, was 29% (range 6%-61%). Of the 18 patients evaluable for inter-compartmental concordance, AB03 had the lowest mutational burden with 19 total variants, whereas AB16 had the highest mutational burden with 86 variants identified (fig.6a)

The number of traceable variants over time is relatively stable and provides useful information about the accuracy of VFC calculations. In all cases, the number of variants calibrated in BM is much greater than the number of these variants subsequently recovered in cfDNA at any timepoint, from as high as 14 variants from AB11 to as few as zero in AB06, who was disqualified from longitudinal analysis for this reason (fig.6b, Table 3)

The ABECMA cohort saw a high number of cfDNA mutations relative to gDNA mutations, including in SHM targets BTG2, BCL6, and CXCR4. However, oncogenes were represented in this cohort, including *TP53, MYC,* and *KRAS* (fig.5b).

Table 3: Number of BM-DSCS-confirmed cfDNA variants available to track over time

Patient	Calibration cfDNA	D+0 cfDNA	D+2 cfDNA	D+7 cfDNA
AB_01	3	2	2	4
AB_02	5	4	3	5
AB_03	2	6	5	3
AB_04	6	2	2	3
AB_05	8	7	8	8
AB_06	2	0	2	3
AB_07	2	2	4	3
AB_08	15	7	14	8
AB_09	3	2	3	2
AB_11	14	14	11	7
AB_12	7	4	5	0
AB_13	2	1	1	1
AB_14	6	NS	NS	NS
AB_15	3	2	0	0
AB_16	12	NS	NS	NS
AB_18	11	10	10	11
AB_19	8	NS	11	9
AB_20	5	NS	NS	NS
NS= No sample collected				

9.4.3   Calibration timepoint comparisons between NDMM and ABECMA cohorts

The variants identified in both cohorts differ with respect to the relative representation of oncogenes compared to SHM targets: in particular, the greater representation of *MYC, TRAF3,* and *TP53* mutations in the ABECMA cohort illustrates this difference, while both cohorts still have high representation of SHM targets such as *BTG2* and *BCL6* (fig.5a and 5b). The ABECMA cohort has more DSCS-confirmed variants detected in bone marrow at the calibration timepoint (though the relationship is not statistically significant, $p > 0.05$, fig.5c), and more of these variants detected using SSCS enumeration in cfDNA ($p < 0.05$, fig. 5d). The VAF of DSCS-calibrated bone marrow variants is much higher in the PA19 cohort than in the Abecma cohort ($p < 0.01$, fig.5e), but there is no significant difference between the VAF of those variants enumerated in cfDNA (fig.5f).

9.4.4 Longitudinal and outcome analysis of ABECMA patients

Due to the recency of CAR-T infusions and median overall survival, long-term outcomes cannot be evaluated. Instead, the major outcome evaluated here is Day 30 IMWG response, dichotomized as Complete Response (CR) or better (stringent Complete Response, sCR); and worse (Very Good Partial Response, VGPR; Partial Response, PR; Stable Disease, SD; and Progressive Disease, PD)[20]. In addition, as the median overall survival was reached, analysis on the basis of survival is included here.

Table 4: VAF and VFC for all patients

Patient Identifier	Day 0 VAF	Day 2 VAF	Day 7 VAF	VAF Fold Change (VFC), D+2, D+0	VAF Fold Change (VFC), D+7, D+0	Survival (days)	D+30 IMWG Outcome
AB01	0.21323	0.22192	0.11577	1.041	0.543	Alive	SD/MR
AB02	0.08248	0.11388	0.06229	1.381	0.755	59	SD/MR
AB03	0.00279	0.00531	0.00156	1.900	0.556	140	VGPR
AB04	0.00183	0.00088	0.00168	0.479	0.916	195	sCR
AB05	0.00308	0.01267	0.00798	4.122	2.594	Alive	sCR
AB06	**FTIC**	0.00012	0.00043	NE	NE	59	PR
AB07	0.00072	0.00049	0.00087	0.681	1.211	128	sCR
AB08	0.01848	0.00812	0.01436	0.439	0.777	Alive	sCR
AB09	0.24753	0.12196	0.01667	0.493	0.067	Alive	sCR
AB10	NS-QC (BM failed QC)	NE	NE	NE	NE	90	SD/MR
AB11	0.03554	0.05377	0.10480	1.513	2.949	14, death due to CAR-T toxicity	N/A
AB12	0.21306	0.17222	NS-QC	0.808	NE	Alive	sCR

AB13	0.00187	0.00884	0.00115	4.731	0.614	42, death not MM-related	SD/MR
AB14	No infusion, deceased	N/A	N/A	N/A	N/A	Unknown	N/A
AB15	0.00054	**FTIC**, 0	**FTIC**, 0	0	0	28	PD
AB16	No infusion, deceased	N/A	N/A	N/A	N/A	Unknown	N/A
AB18	0.02815	0.06998	0.15016	2.146	4.111	Alive	CR
AB19	NS	0.09732	0.12312	NE	NE	Alive	VGPR
FTIC= Failed to identify calibration BM variants NS-QC= No sample, sequencing QC failed NS= no sample provided NE= not evaluable							
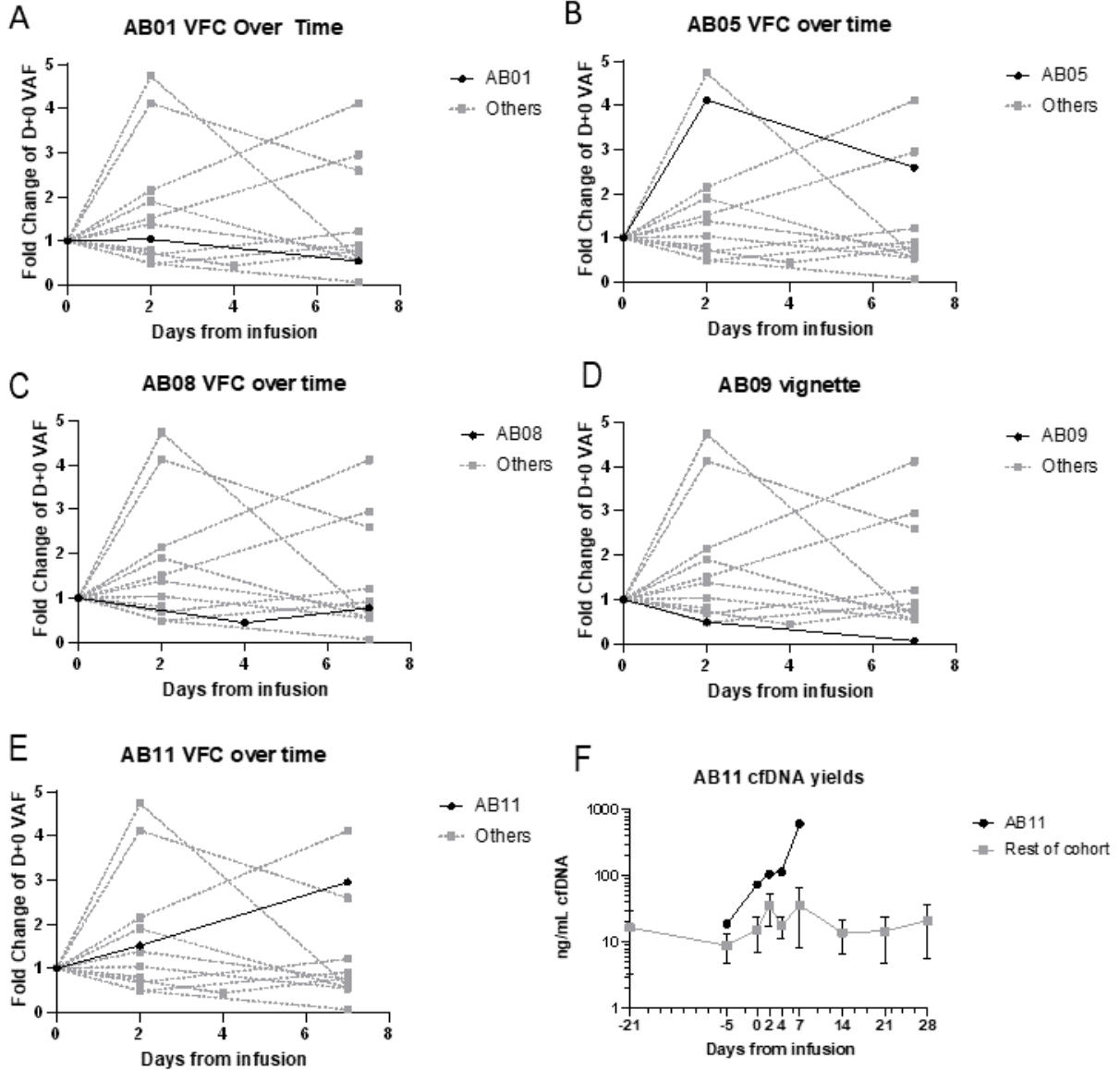
A. AB01 VFC Over Time
B. AB05 VFC over time
C. AB08 VFC over time
D. AB09 vignette
E. AB11 VFC over time
F. AB11 cfDNA yields
G. VAF Fold Change over Time, Coded by D+30 Response

Stringent Complete Response (sCR)
Complete Response (CR)
Very Good Partial Response (VGPR)
Stable Disease/Marginal Response (SD/MR)
Progressive Disease
Deceased
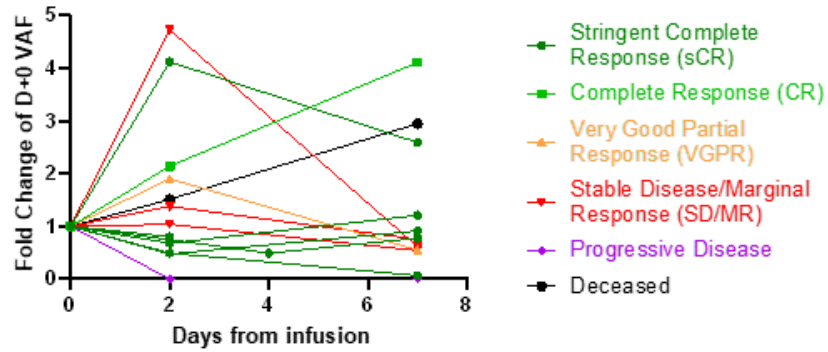
Figure 7: Variant fold change for selected patients A) Variant fold change (VFC) for patient AB01, who had marginal response at D+30. B) VFC for patient AB05, who had a stringent complete response at D+30. C) VFC for patient AB08, who had a stringent complete response at D+30. D) VFC for patient AB09, who had a stringent complete response at D+30. E) VFC for patient AB11, who experienced fatal complications after infusion and died at D+14. F) cfDNA yields per mL of plasma from AB11, who experienced a major spike in cfDNA shedding after infusion. G) VFC for all patients, color-coded by their clinical response at D+30.

9.4.5 AB01, initial SD/MR improving to VGPR by 6 months

Patient AB01 received their infusion in August 2021 and had stable disease (SD/MR) at the D+30 follow-up but was MRD-. By the 3 month follow-up, their assessment improved to a partial response (PR), and by 6 months, to a VGPR with durable survival (still alive at last update). Their VFC rose slightly to 1.041 (median VFC) at D+2 but decreased to 0.543 by D+7 (fig.7a).

9.4.6 AB05, long-term sCR, elevated VFC

Patient AB05 received their infusion in September 2021 and achieved sCR and MRD- by D+30 follow-up, which was sustained out to 6 months after infusion with durable response. Their VFC rose to 4.122 at D+2 and declined slightly to 2.594 by D+7 (fig.7b).

9.4.7 AB08, long-term sCR, depressed VFC

Patient AB08, who had previously received another anti-BCMA therapy, received their infusion in September 2021 and achieved sCR and MRD-by D+30 follow-up, which was sustained out to 6 months after infusion with durable response. Their VFC declined to 0.439 at D+2 before rising slightly to 0.777 by D+7 (fig.7d).

9.4.8 AB09, long-term sCR, depressed VFC

Patient AB09 received their infusion in September 2021 and achieved sCR and MRD- by D+30 follow-up, which was sustained to 6 months after infusion. Their VFC declined to 0.493 at D+2 and 0.067 at D+7 (fig.7d).

9.4.9 AB11, CRS/HLH/Infection, steadily increasing VFC

Patient AB11 received their infusion in September 2021 and experienced major toxicity, autoimmune complications, and infection. They died on D+14 after infusion. The VFC was 1.513 at D+2 and 2.949 at D+7 (fig.7e)

AB11 was unique among their peers in that cfDNA shedding was substantially higher than in the remainder of the cohort, potentially due to the side effects of the CAR-T therapy and associated conditions (fig.7f); however, the VFC steadily rises over time.

9.4.10 Summary of VFC across patients

There is no statistically significant difference between the D+2 VFC in those patients achieving CR or better as opposed to those who did not (Mann-Whitney test, $P=0.1490$), nor was there a difference in the D+7 VFC between these groups (Mann-Whitney test, $P=0.3290$) (fig.8b).

9.4.11 Correspondence between VAF change and outcomes
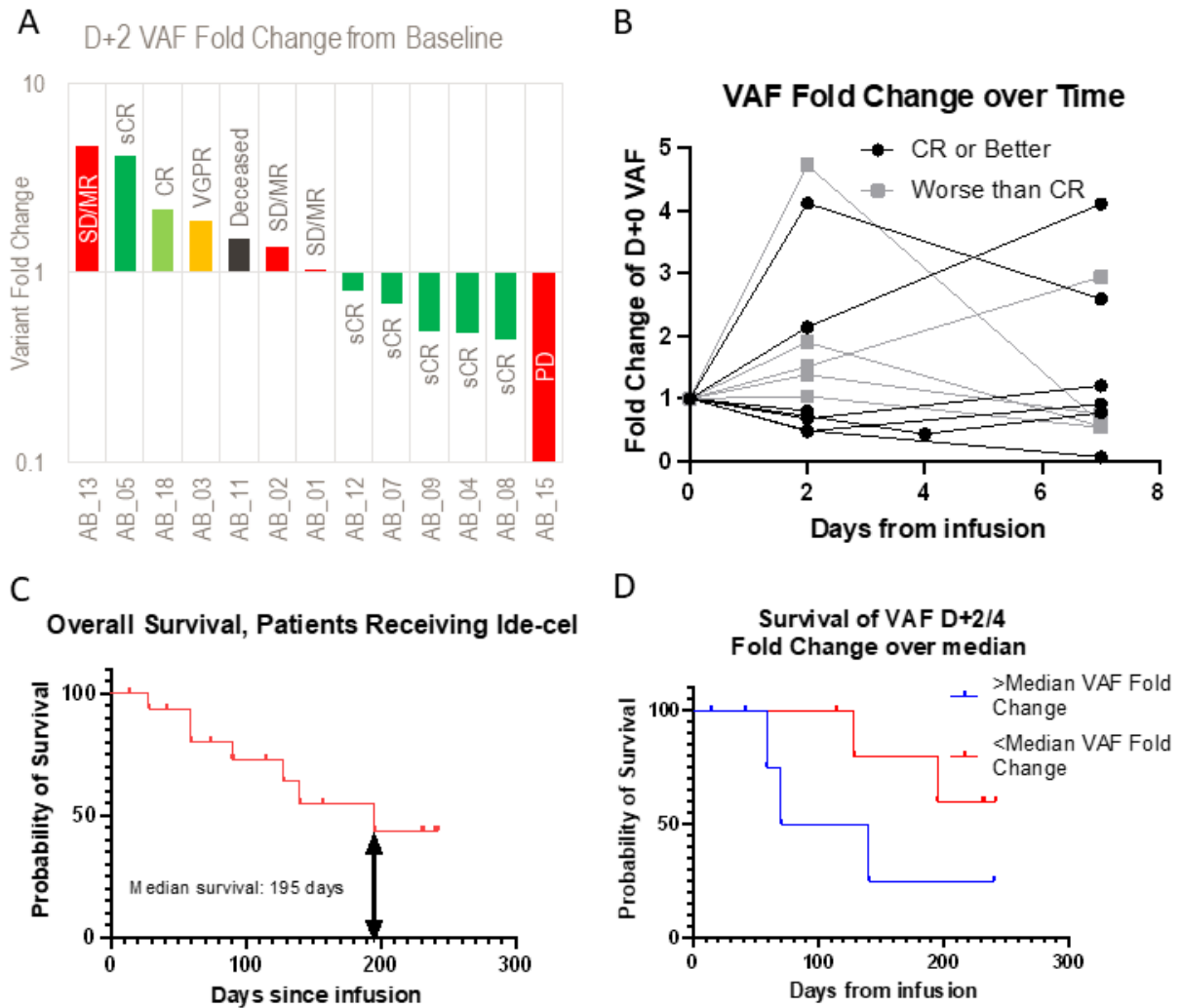
Figure 8: Outcome and survival comparisons with VFC A) Waterfall plot of VFC at D+2, coded by clinical response at D+30. B) VFC for each patient, coded by clinical response at D+30. C) Survival of patients receiving Ide-cel in this cohort. D) Survival of patients in the ABECMA cohort, divided by VFC at D+2.

Evaluable patients were divided into groups based on their VFC at D+2 was greater than or equal to the median VFC or not. Of those patients with ≥Median VFC (n=7), one experienced a D+30 CR, one SCR, one VGPR, three SD/MR, and one patient, AB11, was deceased. Of those with <Median VFC (n=6), five experienced sCR and one experienced

progressive disease (fig.8a). There was no statistically significant difference in the outcomes of these two groups (Fisher's exact test, *P*=0.1026).

As described above, two patients (AB11 and AB13) are censored from survival analysis due to their deaths not being related to MM. The difference in survival between those patients with ≥Median VFC and <Median VFC is not statistically significant (Log-rank *P*=0.1574, fig.8d).

10 **Discussion**

10.1 **Design and performance of M5Seq**

Revision of the MM_M4 panel to M5Seq was performed in order to port the new panel to hg38 for manufacture by Twinstrand Biosciences. In working with specialists at Twinstrand, several regions of the panel were identified which had a high number of off-target BLAST hits, a high $\Delta G°$ of folding, or highly repetitive sequences. Designing probes for this region proved problematic because off-target capture was likely to occur and variants were likely to be spurious true variants, i.e. irrelevant to the tumor. Many of these regions were removed, including several *IGH, IGL,* and *IGK* loci which may have revealed a relevant tumor clonotype.

Revision of the MM_M4 hybrid capture panel led to a meaningful decrease in applicability *in silico:* while the MM_M4 panel had 99.41% applicability, and 90% of tumors had at least 10 variants detected, the M5Seq panel had 97% applicability and 71% of tumors had at least 10 variants detected. However, relative decrease in off-target sequencing, combined with higher on-target rates resulting from the Twinstrand capture protocol, may have mitigated this problem, though this has not been experimentally validated. Analysis of the NDMM samples indicates that true mutation coverage of the panel is much higher (fig.4a), and every patient in both cohorts shown here had more than the *in silico* mode of 6 variants identified in their bone marrow and called by DSCS. This may be due to increased sequencing depth used for the tumors investigated here compared to the WGS-identified variants in the CoMMpass databse and the higher specificity of sequencing resulting from hybrid capture.

10.1.1 Trade-offs of sequencing depth and breadth

There is an inherent trade-off between sequencing breadth and depth: the tumors in the CoMMpass database were sequenced using broad whole genome sequencing or exome sequencing (WES) with sequencing depth one to two orders of magnitude less than the sequencing depth employed in this study. The resulting difference in sensitivity means that in a library with, for example, 200x mean depth should not expect to reliably see rare variants with $oVAF < 5x10^{-3}$, whereas in spike-in libraries with 25,000x mean depth, variants with $oVAF < 5x10^{-5}$ were observed. While exome sequencing should identify variants in a larger selection of the genome, by tiling specifically for regions with high frequency of variants, the CaPP-Seq method preserves as many of the identified variants as possible while ignoring regions where variants are infrequent and likely immaterial to the disease. The additional benefit of the additional depth used in targeted sequencing is the ability to detect changes of VAF over several orders of magnitude, whereas WES is not able to detect low levels of disease with the same amount of sequencing, as observed by Manier et al[45], who use WES in active disease only.

10.1.2 Analytical sensitivity

Sensitivity of a sequencing assay is a function of multiple factors, including sequencing depth, library complexity, and sequencing error rates. Average sequencing depth is the number of reads covering a certain location in the genome and corresponds to the divisor in a calculation of the frequency of a variant, i.e. number of total reads confirming a variant divided by total depth at that variant. The probability of detecting a variant is given by the Poisson distribution, which predicts the likelihood of detecting multiple discrete events. If the true VAF of a variant is greater than the inverse of sequencing depth, then the

probability of detecting the variant is 1; however, if the true VAF of a variant is less than the

sequencing depth, then the probability of detecting it is less than 1 and again predicted using

a Poisson distribution. However, the probability of detecting each variant is additive, so

while the probability of detecting one variant might be very low, if multiple variants are

present, the probability of detecting any variant (and therefore disease burden) is determined

by the frequency of each variant and the number of total variants. Therefore, at low levels of

disease burden, the detection of some variants is certain, but the total number of variants

detected decreases substantially, and the detection a given variant is stochastic. By

sequencing relatively few loci at great depth, we demonstrated an ability to detect variants

using SSCS at an observed VAF of 5×10^{-5}, thus increasing the probability of detecting

variants which are present at lower frequency than the depth of sequencing in other

experiments. As a result, we detect variants at EAF$<10^{-5}$ but no less than oVAF$=5 \times 10^{-5}$, and

these variants are not consistent from dilution series to dilution series, though all are detected

in the calibration sample. In order to detect variants at greater depth consistently, sequencing

depth would need to be increased, and this would likely also improve linearity of the assay as

the oVAF of a low-frequency variant approaches that of its EAF.

Common to all experiments is sequencer and polymerase error: while Illumina

sequencers have error rates on the order of 0.01% (10^{-4})[108], sequencing in excess of 3×10^8

bases per sample, as was the case with each spike-in library, means that 10^4 sequencing

errors will be generated. Additional variant reads will be generated due to polymerase error

during the PCR required for library preparation. The polymerase error rate for the enzyme

used in all the experiments reported here is on the order of 10^{-5}-10^{-6} bases incorporated[109],

adding further sources of error in the library prep. As demonstrated by the SSCS vs DSCS

comparisons in the spike-ins, NDMM, and ABECMA pre-treatment comparisons, PCR and sequencing errors are largely mitigated by DSCS calibration without affecting sensitivity.

Another major factor affecting analytical sensitivity is library complexity, defined as the number of unique molecules in a sequencing library. Library complexity is the result of two factors: total DNA input and conversion rate, or the percentage of molecules successfully converted to library. Using the Twinstrand library preparation protocol, library conversion is 10% for sonicated genomic DNA as used in spike-ins and bone marrow samples, and 30% for cfDNA; as such, more sequencing reads are required to sequence cfDNA samples to the same depth as sonicated gDNA samples. In turn, the best way to increase library complexity is to increase sample DNA input whenever possible. The samples sequenced here were limited to a maximum of 250ng sonicated gDNA, 100ng cfDNA for pre-treatment samples, and 50ng for longitudinal samples; however, this limit was infrequently achieved, especially in NDMM pre-treatment samples when disease burden and cfDNA shedding was low. In instances where cfDNA shedding is high, while libraries can be made from >1500ng DNA, sequencing costs to achieve necessary depth rapidly cause sequencing to become uneconomical. In sum, the limiting factor of the sensitivity of the assay is DNA input, as demonstrated by the spike-in experiments: by using 1500ng DNA input, we sequenced 500,000 haploid genome equivalents to an average depth of ~20,000x. In contrast, 100ng cfDNA input is equivalent to 33,000 haploid genome equivalents at 10,000x depth, and low-input samples of 30ng are equivalent to 10,000 haploid genome equivalents at 5,000x depth. Here, we sought to strike a balance between economy of sequencing, sequencing depth, and library complexity.

As shown in figure 3c and 3d, calling variants using DSCS in all spike-in libraries is insufficient to detect low frequency variants at less than 10^{-4}. This is due to the considerations listed above, chiefly that when using DSCS variant calling, a failure to reconcile paired reverse complement strands leads to a loss of average variant depth and resulting loss of sensitivity (fig.3e). However, this is rescued by calling variants in the calibration sample in duplex to mitigate sequencing error, thus contributing confidence to variant calls, and then only requiring single strand support for the variant in successive samples, as shown in figures 3a and 3b. Due to the increased variant depth when using SSCS, variants are called at VAF as low as 5×10^{-5}. Analysis when using SSCS exclusively, even for calibration, does lead to a great deal of expected genomic noise which confounds data analysis.

As shown in figures 3a and 3b, linearity on a logarithmic scale is lost at an EAF of 10^{-4} for both the U266 and H929 spike-ins. Loss of linearity indicates that a variant's OAF, if quantitated at $<10^{-4}$ indicates that the true VAF is $<10^{-4}$ but cannot be accurately quantified. This is similar to a common result in ASO-qPCR MRD assays, which may return a result of "Positive, Non-Quantifiable" (PNQ). A PNQ result is still useful for detecting low-level disease and molecular response.

Due to the combination of loss of linearity at 10^{-4}, limit of sensitivity of 5×10^{-5}, and practical considerations such as library complexity, the limit of sensitivity of the assay in clinical practice is likely less than demonstrated here, and therefore may not accurately measure MRD at the limit of sensitivity demonstrated by clonoSEQ or MFC-based assays. However, this analysis has specifically excluded plasma samples that are contemporaneous with MRD measurements: in particular, at D+28/D+30 from CAR-T infusion for the

ABECMA cohort. As the majority of patients were MRD- at D+30 (Table #1), it may be informative to interrogate these samples for VFC at the D+30 timepoint, as was done by Deng *et al*[118], especially since several MRD- patients relapsed after D+30. However, given the small sample size, it is possible that this cohort would not be informative. More investigation, including a mature cohort with multiple long-term survivors, is needed to investigate the true utility of this assay for MRD detection purposes.

10.2 Applications

10.2.1 Variant filtering in the absence of a matched normal sample

Like any NGS assay, hybrid capture assays are challenged by the need to ascertain what is a germline variant and what is a tumor-derived variant. The CaPP-Seq method and its iterations typically requires the use of a matched normal sample for every patient as a part of the calibration step in order to remove germline variants: the normal sample, usually PBMC, is sequenced at less depth than the clinical sample in order to identify obvious germline variants. While this is the standard practice for CaPP-Seq assays, it has two weaknesses: first, removing only biallelic and heterozygous variants may leave behind low-frequency germline variants and off-target non-tumor SHM variants, which when included in VAF calculations may skew VAF calculations as the tumor-derived VAF changes over time; alternately, inclusion of low-frequency variants in blacklists may cause true tumor variants to be blacklisted. Another alternative which minimizes sequencing cost is to perform low-pass whole genome sequencing (lpWGS) in order to estimate tumor purity, and therefore establishing a VAF threshold based on the tumor purity.

These experiments did not use a matched normal sample, so analysis is, strictly speaking, ignorant of germline variants. The stringent filtering strategy used here involved using multiple compendia of population-level mutational databases to eliminate common variants and repetitive elements, and the average VAF in patient samples is reflective of this: the average VAF for each patient is >0.1 (table 3). However, it is likely that several true tumor-derived variants were lost in this filtering step, potentially negatively affecting the utility of this assay by blunting its sensitivity to detect VAF changes.

This is particularly apparent when comparing the DSCS and SSCS consensus pre-treatment comparisons of both cohorts, as there is not a substantive increase in concordant variants by using SSCS in many cases, and in fact, the median concordance decreases (29% in DSCS vs 14% with SSCS in the ABECMA cohort), and slightly fewer variants are called in the SSCS data than in the DSCS data (median 45.5 vs 38.5). This suggests that the plan of tracking SSCS-confirmed variants calibrated in DSCS BM may not achieve the increased sensitivity and applicability, as approximated by number of SSCS-supported, DSCS-BM calibrated variants. However, this problem may be attributed to the filtering step, as analyses which do not use the dbSNP and repeatMasker annotations, but which do use PAF and the PoN, do not suffer from this issue. For M5Seq to be incorporated into a clinical setting, this process will need major refinement. Alternatives to the dbSNP and repeatMasker steps include using a matched normal sample with a conservative VAF cutoff (e.g., blacklist anything with VAF>0.4), or limiting analysis in the absence of a normal sample to variants below a VAF "cap" above which threshold variants are not included in longitudinal analysis. This may be done directly through analysis of the pre-treatment BM captured library, or

indirectly via lpWGS and tumor fraction estimation of the pre-capture library for the same sample.

10.2.2 Inter-sample concordance and implications of low concordance

Concordance between the pre-treatment NDMM sample compartments, using DSCS, was generally fair. All tumors presented more variants than the average number of variants detected in the *in silico* validation cohort (11.89), but the median concordance was <25%, and the resulting low number of concordant variants decreases the probability of detecting low disease burden. For instance, at a given VAF, MM0018 and MM0012 have a lower probability of detecting variants than do MM0015 and MM0031 due to the difference in concordant variants. Moreover, the inability to detect concordant variants in the cfDNA of two patients (MM0014 and MM0019) using DSCS indicates the limitations of this approach, as no mutations could be followed longitudinally with high confidence in these patients.

However, the benefit of switching to SSCS confirmation of calibrated variants is not clear in this cohort as was anticipated. The SSCS data indicate a preponderance of variants in all samples, but concordance does not improve overall, and while MM0018 is rescued (5 concordant variants, as opposed to 0 in the DSCS comparison), MM0014 still has no concordant variants and, uniquely, MM0018 loses their concordance.

Taken together, this approach demonstrates the limitations of this approach when stringently filtering variants, as concordance is low and likely true tumor variants are blacklisted from analysis.

10.2.3 Challenges of subsampling in M5Seq

cfDNA sequencing is an attempt to reproduce the local features of a primary tumor in a global compartment- as such, a subsample is being taken which may not perfectly represent the primary tumor, as we and others show. If we assume, for instance, that an average plasma sample from a 10mL blood tube contains 50ng of DNA (at 10ng cfDNA/mL plasma), then we are sampling roughly 7,600 haploid genome equivalents from a total of nearly 3.8 million genome equivalents, a proportion of 1/500. Variant molecules which are not present at a frequency of greater than 3/500 (due to the "rule of three" in Poisson sampling) have a chance of being sampled of <1. From there, the molecules must be extracted from the plasma and turned into library molecules, which has efficiency of <50%. From there, it must be captured and sequenced. In this light, increased cfDNA input into library construction is the factor which has the greatest impact on the ability to detect rare variants, and this may come from higher cfDNA burden in plasma or from multiple blood tubes. While subsampling is unavoidable, hybrid capture maximizes the probability of detecting tumor-derived molecules if they make it through these multiple subsampling steps.

10.3 Applications in CAR-T therapy

10.3.1 Inter-compartment concordance in CAR-T patients has not been studied

Consistent with the analysis of NDMM samples, concordance between pre-treatment cfDNA and bone marrow samples is low, with fewer than 30% of variants identified in both pre-treatment compartments using DSCS. This is an improvement compared to PA19 samples, and is likely due to the greater mutational burden. While more variants are called, on average, in the ABECMA cohort, the lack of concordance is consistent with the PA19

61

samples. Unlike the PA19 samples, however, is the reliability of the SSCS data. Nevertheless, concordance actually decreases overall, and fewer variants are called overall. This further challenges the idea that SSCS confirmation of DSCS-calibrated variants increases sensitivity. While there is still high confidence that the concordant variants called are true variants which can be followed over time, it is again likely that true tumor variants are being blacklisted in this analysis.

10.3.2 VFC may predict outcomes within 2/7 days

These experiments identified trends between VFC at D+2 and IMWG response at D+30; however, these trends did not rise to the level of statistical significance. Indeed, while the majority of CR patients had a decrease in VFC by D+2, this trend was not stastically significant. Concerningly, in multiple instances patients (AB05 and AB18) achieved sCR and, in the case of AB05 (AB18 only received infusion in January 2022), experienced prolonged survival despite an elevated VCF at both D+2 and D+7. These data indicate that M5Seq alone cannot prognosticate survival given the limitations of this study; however, additional experimentation may be warranted to demonstrate the efficacy of M5Seq. Patients AB05 and AB18 demonstrate a paradoxical "spike" in VAF at D+2, which has been documented in literature previously, though not in the context of CAR-T therapy- to our knowledge, this represents the first observation of a ctDNA spike in CAR-T therapy. In myeloma, the spike has been observed 3-5 days following standard chemotherapy, but investigators found it to be inconsistent when using captured sequencing[123]. The presence of the spike has been suggested [124] to be demonstrative of sustained anti-tumor activity of the therapeutic agent over the days following treatment, but the fact that the spike is only present in a minority of cases suggests that this is not the whole story. Moreover, in the

context of short-term response, this needs to be adequately controlled for and understood when assessing short term response.

10.3.3 Clinical application of M5Seq

Here, we demonstrated that M5Seq has sufficient analytical sensitivity and applicability to detect low-frequency variants but may lack the prognostic power necessary to accurately predict response to CAR-T therapy through the use of ctDNA, hybrid capture, and massively parallel sequencing. However, the small sample size available may justify further study to see whether statistical significance is hindered by the number of patients. While assays exist for MM which use liquid biopsies, and/or hybrid capture and massively parallel sequencing, these assays are primarily designed for detection of MRD, and no such assays are designed for use in a dynamic treatment environment.

Given sensitivity, specificity, applicability, and qualified ability of M5Seq to prognosticate outcomes, M5Seq may provide some clinical utility to investigators in assessing CAR-T response in MM. Given the recent approval and improvements in outcomes in cilta-cel patients compared to ide-cel patients, M5Seq may identify changes in molecular response between the two treatment groups, which in turn may establish the superiority of one therapy over another. In addition, the efficacy of CAR-T therapy advocates for its use in treatment settings less advanced than relapsed/refractory MM, and molecular response may play a greater role in predicting outcomes in that treatment setting.

10.4 Future Directions

While ctDNA is a promising avenue for investigating response to MM therapy in a dynamic range, the biological reality of lymphoid malignancies is complex and may be better

served using a multimodal approach. Deng *et al* integrated molecular response data with single-cell transcriptomic and immunologic features of axicabtagene ciloleucel (axi-cel) infusion products, finding that the molecular response corresponded to the fraction of exhausted CD8+ T cells in the infusion product, thus suggesting that the efficacy of axi-cel therapy can be influenced by the health of the T-cell repertoire at apheresis, and limited tumor biopsies supported these results. Similarly, the data reported here are one element of a larger project investigating responses to ide-cel, both in bone marrow and in cfDNA. Work is underway to assess single-cell transcriptomic and immunologic features of the primary tumors sequenced here in order to similarly integrate these data and better understand how and why ide-cel fails.

Another promising avenue for this project is the integration of low-pass whole genome sequencing (lpWGS). lpWGS identifies high-level chromosomal defects such as deletions and hyperdiploidies at low cost due to the low sequencing coverage required, and the magnitude of these defects is indicative of disease burden in MM[45]. Moreover, our group demonstrated recently that in DLBCL, lpWGS carries prognostic value and is able to stratify patients on risk of relapse after axi-cel based on pre-infusion cfDNA samples[93]. Sequencing pre-infusion cfDNA in this manner may further the idea that cfDNA is prognostic for CAR-T response. In addition, the lpWGS results from bone marrow can be used to estimate tumor purity, which can then be used to determine a VAF cutoff for filtering non-tumor variants when applying M5Seq to the same tumors. Using the same protocols used here, lpWGS libraries may be generated without any extra work, as a diluted aliquot of library taken for QC before capture contains sufficient DNA to perform lpWGS.

It is notable that the median OS in this cohort underachieves when compared to the KarMMa trial cohorts which engendered FDA approval of ide-cel (fig.8c)[14, 15]. This cohort may have failed to perfectly represent patients receiving ide-cel, and as new patients continue to receive ide-cel, continuous evaluation of survival and molecular response may display improved survival and better prognostic ability. In short, the use of M5Seq in broader patient cohorts may reveal greater utility. Furthermore, promising results from the CARTITUDE trials and recent FDA approval of anti-BCMA ciltacabtagene autoleucel (cilta-cel) provide a treatment which may be studied in comparison and competition with ide-cel, and utilizing M5Seq to assess molecular response can contribute to comparative studies of the two myeloma CAR-T products.

11 Bibliography

1.	Kyle, R.A. and S.V. Rajkumar, *Multiple myeloma.* Blood, 2008. **111**(6): p. 2962-72.

2.	Kyle, R.A., T.M. Therneau, S.V. Rajkumar, D.R. Larson, M.F. Plevak, and L.J. Melton, 3rd, *Incidence of multiple myeloma in Olmsted County, Minnesota: Trend over 6 decades.* Cancer, 2004. **101**(11): p. 2667-74.

3.	Kyle, R.A., M.A. Gertz, T.E. Witzig, J.A. Lust, M.Q. Lacy, A. Dispenzieri, R. Fonseca, S.V. Rajkumar, J.R. Offord, D.R. Larson, M.E. Plevak, T.M. Therneau, and P.R. Greipp, *Review of 1027 patients with newly diagnosed multiple myeloma.* Mayo Clin Proc, 2003. **78**(1): p. 21-33.

4.	Manier, S., K.Z. Salem, J. Park, D.A. Landau, G. Getz, and I.M. Ghobrial, *Genomic complexity of multiple myeloma and its clinical implications.* Nat Rev Clin Oncol, 2017. **14**(2): p. 100-113.

5.	Chapman, M.A., M.S. Lawrence, J.J. Keats, K. Cibulskis, C. Sougnez, A.C. Schinzel, C.L. Harview, J.P. Brunet, G.J. Ahmann, M. Adli, K.C. Anderson, K.G. Ardlie, D. Auclair, A. Baker, P.L. Bergsagel, B.E. Bernstein, Y. Drier, R. Fonseca, S.B. Gabriel, C.C. Hofmeister, S. Jagannath, A.J. Jakubowiak, A. Krishnan, J. Levy, T. Liefeld, S. Lonial, S. Mahan, B. Mfuko, S. Monti, L.M. Perkins, R. Onofrio, T.J. Pugh, S.V. Rajkumar, A.H. Ramos, D.S. Siegel, A. Sivachenko, A.K. Stewart, S. Trudel, R. Vij, D. Voet, W. Winckler, T. Zimmerman, J. Carpten, J. Trent, W.C. Hahn, L.A. Garraway, M. Meyerson, E.S. Lander, G. Getz, and T.R. Golub, *Initial genome sequencing and analysis of multiple myeloma.* Nature, 2011. **471**(7339): p. 467-72.

6.	Lohr, J.G., P. Stojanov, S.L. Carter, P. Cruz-Gordillo, M.S. Lawrence, D. Auclair, C. Sougnez, B. Knoechel, J. Gould, G. Saksena, K. Cibulskis, A. McKenna, M.A.

Chapman, R. Straussman, J. Levy, L.M. Perkins, J.J. Keats, S.E. Schumacher, M. Rosenberg, C. Multiple Myeloma Research, G. Getz, and T.R. Golub, *Widespread genetic heterogeneity in multiple myeloma: implications for targeted therapy.* Cancer Cell, 2014. **25**(1): p. 91-101.

7.   Segges, P., E. Braggio, C. Minnicelli, R. Hassan, I.R. Zalcberg, and A. Maiolino, *Genetic aberrations in multiple myeloma characterized by cIg-FISH: a Brazilian context.* Braz J Med Biol Res, 2016. **49**(5): p. e5034.

8.   Pasqualucci, L., P. Neumeister, T. Goossens, G. Nanjangud, R.S. Chaganti, R. Kuppers, and R. Dalla-Favera, *Hypermutation of multiple proto-oncogenes in B-cell diffuse large-cell lymphomas.* Nature, 2001. **412**(6844): p. 341-6.

9.   Alvarez-Prado, A.F., P. Perez-Duran, A. Perez-Garcia, A. Benguria, C. Torroja, V.G. de Yebenes, and A.R. Ramiro, *A broad atlas of somatic hypermutation allows prediction of activation-induced deaminase targets.* J Exp Med, 2018. **215**(3): p. 761-771.

10.   Kyle, R.A., *The monoclonal gammopathies.* Clin Chem, 1994. **40**(11 Pt 2): p. 2154-61.

11.   Tosi, P., S. Tomassetti, A. Merli, and V. Polli, *Serum free light-chain assay for the detection and monitoring of multiple myeloma and related conditions.* Ther Adv Hematol, 2013. **4**(1): p. 37-41.

12.   Anderson, K.C., *Progress and Paradigms in Multiple Myeloma.* Clin Cancer Res, 2016. **22**(22): p. 5419-5427.

13.   Martinez-Lopez, J., B. Paiva, L. Lopez-Anglada, M.V. Mateos, T. Cedena, M.B. Vidriales, M.A. Saez-Gomez, T. Contreras, A. Oriol, I. Rapado, A.I. Teruel, L.

Cordon, M.J. Blanchard, E. Bengoechea, L. Palomera, F. de Arriba, C. Cueto-Felgueroso, A. Orfao, J. Blade, J.F. San Miguel, J.J. Lahuerta, and G. Spanish Multiple Myeloma Group / Program for the Study of Malignant Blood Diseases Therapeutics Cooperative Study, *Critical analysis of the stringent complete response in multiple myeloma: contribution of sFLC and bone marrow clonality.* Blood, 2015. **126**(7): p. 858-62.

14.   Munshi, N.C., L.D. Anderson, Jr., N. Shah, D. Madduri, J. Berdeja, S. Lonial, N. Raje, Y. Lin, D. Siegel, A. Oriol, P. Moreau, I. Yakoub-Agha, M. Delforge, M. Cavo, H. Einsele, H. Goldschmidt, K. Weisel, A. Rambaldi, D. Reece, F. Petrocca, M. Massaro, J.N. Connarn, S. Kaiser, P. Patel, L. Huang, T.B. Campbell, K. Hege, and J. San-Miguel, *Idecabtagene Vicleucel in Relapsed and Refractory Multiple Myeloma.* N Engl J Med, 2021. **384**(8): p. 705-716.

15.   Raje, N., J. Berdeja, Y. Lin, D. Siegel, S. Jagannath, D. Madduri, M. Liedtke, J. Rosenblatt, M.V. Maus, A. Turka, L.P. Lam, R.A. Morgan, K. Friedman, M. Massaro, J. Wang, G. Russotti, Z. Yang, T. Campbell, K. Hege, F. Petrocca, M.T. Quigley, N. Munshi, and J.N. Kochenderfer, *Anti-BCMA CAR T-Cell Therapy bb2121 in Relapsed or Refractory Multiple Myeloma.* N Engl J Med, 2019. **380**(18): p. 1726-1737.

16.   Berdeja, J.G., D. Madduri, S.Z. Usmani, A. Jakubowiak, M. Agha, A.D. Cohen, A.K. Stewart, P. Hari, M. Htut, A. Lesokhin, A. Deol, N.C. Munshi, E. O'Donnell, D. Avigan, I. Singh, E. Zudaire, T.M. Yeh, A.J. Allred, Y. Olyslager, A. Banerjee, C.C. Jackson, J.D. Goldberg, J.M. Schecter, W. Deraedt, S.H. Zhuang, J. Infante, D. Geng, X. Wu, M.J. Carrasco-Alfonso, M. Akram, F. Hossain, S. Rizvi, F. Fan, Y. Lin, T.

Martin, and S. Jagannath, *Ciltacabtagene autoleucel, a B-cell maturation antigen-directed chimeric antigen receptor T-cell therapy in patients with relapsed or refractory multiple myeloma (CARTITUDE-1): a phase 1b/2 open-label study.* Lancet, 2021. **398**(10297): p. 314-324.

17.   Rawstron, A.C., W.M. Gregory, R.M. de Tute, F.E. Davies, S.E. Bell, M.T. Drayson, G. Cook, G.H. Jackson, G.J. Morgan, J.A. Child, and R.G. Owen, *Minimal residual disease in myeloma by flow cytometry: independent prediction of survival benefit per log reduction.* Blood, 2015. **125**(12): p. 1932-5.

18.   Martinez-Lopez, J., J.J. Lahuerta, F. Pepin, M. Gonzalez, S. Barrio, R. Ayala, N. Puig, M.A. Montalban, B. Paiva, L. Weng, C. Jimenez, M. Sopena, M. Moorhead, T. Cedena, I. Rapado, M.V. Mateos, L. Rosinol, A. Oriol, M.J. Blanchard, R. Martinez, J. Blade, J. San Miguel, M. Faham, and R. Garcia-Sanz, *Prognostic value of deep sequencing method for minimal residual disease detection in multiple myeloma.* Blood, 2014. **123**(20): p. 3073-9.

19.   Gozzetti, A., D. Raspadori, F. Bacchiarri, A. Sicuranza, P. Pacelli, I. Ferrigno, D. Tocci, and M. Bocchia, *Minimal Residual Disease in Multiple Myeloma: State of the Art and Applications in Clinical Practice.* J Pers Med, 2020. **10**(3).

20.   Kumar, S., B. Paiva, K.C. Anderson, B. Durie, O. Landgren, P. Moreau, N. Munshi, S. Lonial, J. Blade, M.V. Mateos, M. Dimopoulos, E. Kastritis, M. Boccadoro, R. Orlowski, H. Goldschmidt, A. Spencer, J. Hou, W.J. Chng, S.Z. Usmani, E. Zamagni, K. Shimizu, S. Jagannath, H.E. Johnsen, E. Terpos, A. Reiman, R.A. Kyle, P. Sonneveld, P.G. Richardson, P. McCarthy, H. Ludwig, W. Chen, M. Cavo, J.L. Harousseau, S. Lentzsch, J. Hillengass, A. Palumbo, A. Orfao, S.V. Rajkumar, J.S.

Miguel, and H. Avet-Loiseau, *International Myeloma Working Group consensus criteria for response and minimal residual disease assessment in multiple myeloma.* Lancet Oncol, 2016. **17**(8): p. e328-e346.

21.   Mailankody, S., N. Korde, A.M. Lesokhin, N. Lendvai, H. Hassoun, M. Stetler-Stevenson, and O. Landgren, *Minimal residual disease in multiple myeloma: bringing the bench to the bedside.* Nat Rev Clin Oncol, 2015. **12**(5): p. 286-95.

22.   Paiva, B., N. Puig, M.T. Cedena, L. Rosinol, L. Cordon, M.B. Vidriales, L. Burgos, J. Flores-Montero, L. Sanoja-Flores, L. Lopez-Anglada, R. Maldonado, J. de la Cruz, N.C. Gutierrez, M.J. Calasanz, M.L. Martin-Ramos, R. Garcia-Sanz, J. Martinez-Lopez, A. Oriol, M.J. Blanchard, R. Rios, J. Martin, R. Martinez-Martinez, A. Sureda, M.T. Hernandez, J. de la Rubia, I. Krsnik, J.M. Moraleda, L. Palomera, J. Bargay, J.J.M. Van Dongen, A. Orfao, M.V. Mateos, J. Blade, J.F. San-Miguel, J.J. Lahuerta, and G.P.C.S. Group, *Measurable Residual Disease by Next-Generation Flow Cytometry in Multiple Myeloma.* J Clin Oncol, 2020. **38**(8): p. 784-792.

23.   Kurtz, D.M., M.R. Green, S.V. Bratman, F. Scherer, C.L. Liu, C.A. Kunder, K. Takahashi, C. Glover, C. Keane, S. Kihira, B. Visser, J. Callahan, K.A. Kong, M. Faham, K.S. Corbelli, D. Miklos, R.H. Advani, R. Levy, R.J. Hicks, M. Hertzberg, R.S. Ohgami, M.K. Gandhi, M. Diehn, and A.A. Alizadeh, *Noninvasive monitoring of diffuse large B-cell lymphoma by immunoglobulin high-throughput sequencing.* Blood, 2015. **125**(24): p. 3679-87.

24.   Perrot, A., V. Lauwers-Cances, J. Corre, N. Robillard, C. Hulin, M.L. Chretien, T. Dejoie, S. Maheo, A.M. Stoppa, B. Pegourie, L. Karlin, L. Garderet, B. Arnulf, C. Doyen, N. Meuleman, B. Royer, J.R. Eveillard, L. Benboubker, M. Dib, O. Decaux,

A. Jaccard, K. Belhadj, S. Brechignac, B. Kolb, C. Fohrer, M. Mohty, M. Macro, P.G. Richardson, V. Carlton, M. Moorhead, T. Willis, M. Faham, K.C. Anderson, J.L. Harousseau, X. Leleu, T. Facon, P. Moreau, M. Attal, H. Avet-Loiseau, and N. Munshi, *Minimal residual disease negativity using deep sequencing is a major prognostic factor in multiple myeloma.* Blood, 2018. **132**(23): p. 2456-2464.

25.   Munshi, N.C., H. Avet-Loiseau, K.C. Anderson, P. Neri, B. Paiva, M. Samur, M. Dimopoulos, M. Kulakova, A. Lam, M. Hashim, J. He, B. Heeg, J. Ukropec, J. Vermeulen, S. Cote, and N. Bahlis, *A large meta-analysis establishes the role of MRD negativity in long-term survival outcomes in patients with multiple myeloma.* Blood Adv, 2020. **4**(23): p. 5988-5999.

26.   Rawstron, A.C., F.E. Davies, R. DasGupta, A.J. Ashcroft, R. Patmore, M.T. Drayson, R.G. Owen, A.S. Jack, J.A. Child, and G.J. Morgan, *Flow cytometric disease monitoring in multiple myeloma: the relationship between normal and neoplastic plasma cells predicts outcome after transplantation.* Blood, 2002. **100**(9): p. 3095-100.

27.   Rawstron, A.C., B. Kennedy, P.A. Evans, F.E. Davies, S.J. Richards, A.P. Haynes, N.H. Russell, G. Hale, G.J. Morgan, A.S. Jack, and P. Hillmen, *Quantitation of minimal disease levels in chronic lymphocytic leukemia using a sensitive flow cytometric assay improves the prediction of outcome and can be used to optimize therapy.* Blood, 2001. **98**(1): p. 29-35.

28.   Paiva, B., M.B. Vidriales, J. Cervero, G. Mateo, J.J. Perez, M.A. Montalban, A. Sureda, L. Montejano, N.C. Gutierrez, A. Garcia de Coca, N. de Las Heras, M.V. Mateos, M.C. Lopez-Berges, R. Garcia-Boyero, J. Galende, J. Hernandez, L.

Palomera, D. Carrera, R. Martinez, J. de la Rubia, A. Martin, J. Blade, J.J. Lahuerta, A. Orfao, J.F. San Miguel, and G.P.C.S. Groups, *Multiparameter flow cytometric remission is the most relevant prognostic factor for multiple myeloma patients who undergo autologous stem cell transplantation.* Blood, 2008. **112**(10): p. 4017-23.

29.   Flores-Montero, J., L. Sanoja-Flores, B. Paiva, N. Puig, O. Garcia-Sanchez, S. Bottcher, V.H.J. van der Velden, J.J. Perez-Moran, M.B. Vidriales, R. Garcia-Sanz, C. Jimenez, M. Gonzalez, J. Martinez-Lopez, A. Corral-Mateos, G.E. Grigore, R. Fluxa, R. Pontes, J. Caetano, L. Sedek, M.C. Del Canizo, J. Blade, J.J. Lahuerta, C. Aguilar, A. Barez, A. Garcia-Mateo, J. Labrador, P. Leoz, C. Aguilera-Sanz, J. San-Miguel, M.V. Mateos, B. Durie, J.J.M. van Dongen, and A. Orfao, *Next Generation Flow for highly sensitive and standardized detection of minimal residual disease in multiple myeloma.* Leukemia, 2017. **31**(10): p. 2094-2103.

30.   Roshal, M., J.A. Flores-Montero, Q. Gao, M. Koeber, J. Wardrope, B.G.M. Durie, A. Dogan, A. Orfao, and O. Landgren, *MRD detection in multiple myeloma: comparison between MSKCC 10-color single-tube and EuroFlow 8-color 2-tube methods.* Blood Adv, 2017. **1**(12): p. 728-732.

31.   Mathis, S., N. Chapuis, J. Borgeot, M. Maynadie, M. Fontenay, M.C. Bene, J. Guy, and V. Bardet, *Comparison of cross-platform flow cytometry minimal residual disease evaluation in multiple myeloma using a common antibody combination and analysis strategy.* Cytometry B Clin Cytom, 2015. **88**(2): p. 101-9.

32.   Kalina, T., J. Flores-Montero, V.H. van der Velden, M. Martin-Ayuso, S. Bottcher, M. Ritgen, J. Almeida, L. Lhermitte, V. Asnafi, A. Mendonca, R. de Tute, M. Cullen, L. Sedek, M.B. Vidriales, J.J. Perez, J.G. te Marvelde, E. Mejstrikova, O. Hrusak, T.

Szczepanski, J.J. van Dongen, A. Orfao, and C. EuroFlow, *EuroFlow standardization of flow cytometer instrument settings and immunophenotyping protocols.* Leukemia, 2012. **26**(9): p. 1986-2010.

33.   Dimopoulos, M.A., L.A. Moulopoulos, I. Datseris, D. Weber, K. Delasalle, D. Gika, and R. Alexanian, *Imaging of myeloma bone disease--implications for staging, prognosis and follow-up.* Acta Oncol, 2000. **39**(7): p. 823-7.

34.   Bartel, T.B., J. Haessler, T.L. Brown, J.D. Shaughnessy, Jr., F. van Rhee, E. Anaissie, T. Alpe, E. Angtuaco, R. Walker, J. Epstein, J. Crowley, and B. Barlogie, *F18-fluorodeoxyglucose positron emission tomography in the context of other imaging techniques and prognostic factors in multiple myeloma.* Blood, 2009. **114**(10): p. 2068-76.

35.   Nanni, C. and E. Zamagni, *Fluorodeoxyglucose-PET/Computed Tomography as a Predictor of Prognosis in Multiple Myeloma.* PET Clin, 2019. **14**(3): p. 383-389.

36.   Zamagni, E., F. Patriarca, C. Nanni, B. Zannetti, E. Englaro, A. Pezzi, P. Tacchetti, S. Buttignol, G. Perrone, A. Brioli, L. Pantani, C. Terragna, F. Carobolante, M. Baccarani, R. Fanin, S. Fanti, and M. Cavo, *Prognostic relevance of 18-F FDG PET/CT in newly diagnosed multiple myeloma patients treated with up-front autologous transplantation.* Blood, 2011. **118**(23): p. 5989-95.

37.   Dimitrakopoulou-Strauss, A., M. Hoffmann, R. Bergner, M. Uppenkamp, U. Haberkorn, and L.G. Strauss, *Prediction of progression-free survival in patients with multiple myeloma following anthracycline-based chemotherapy based on dynamic FDG-PET.* Clin Nucl Med, 2009. **34**(9): p. 576-84.

38.   Haznedar, R., S.Z. Aki, O.U. Akdemir, Z.N. Ozkurt, O. Ceneli, M. Yagci, G.T. Sucak, and M. Unlu, *Value of 18F-fluorodeoxyglucose uptake in positron emission tomography/computed tomography in predicting survival in multiple myeloma.* Eur J Nucl Med Mol Imaging, 2011. **38**(6): p. 1046-53.

39.   Han, S., S. Woo, Y.I. Kim, D.H. Yoon, and J.S. Ryu, *Prognostic value of (18)F-fluorodeoxyglucose positron emission tomography/computed tomography in newly diagnosed multiple myeloma: a systematic review and meta-analysis.* Eur Radiol, 2021. **31**(1): p. 152-162.

40.   Lutje, S., J.W. de Rooy, S. Croockewit, E. Koedam, W.J. Oyen, and R.A. Raymakers, *Role of radiography, MRI and FDG-PET/CT in diagnosing, staging and therapeutical evaluation of patients with multiple myeloma.* Ann Hematol, 2009. **88**(12): p. 1161-8.

41.   Derlin, T., C. Weber, C.R. Habermann, J. Herrmann, C. Wisotzki, F. Ayuk, C. Wolschke, S. Klutmann, and N. Kroger, *18F-FDG PET/CT for detection and localization of residual or recurrent disease in patients with multiple myeloma after stem cell transplantation.* Eur J Nucl Med Mol Imaging, 2012. **39**(3): p. 493-500.

42.   Rawstron, A.C., R.G. Owen, F.E. Davies, R.J. Johnson, R.A. Jones, S.J. Richards, P.A. Evans, J.A. Child, G.M. Smith, A.S. Jack, and G.J. Morgan, *Circulating plasma cells in multiple myeloma: characterization and correlation with disease stage.* Br J Haematol, 1997. **97**(1): p. 46-55.

43.   Kamande, J.W., M.A.M. Lindell, M.A. Witek, P.M. Voorhees, and S.A. Soper, *Isolation of circulating plasma cells from blood of patients diagnosed with clonal*

plasma cell disorders using cell selection microfluidics. Integr Biol (Camb), 2018. **10**(2): p. 82-91.

44. Vij, R., A. Mazumder, M. Klinger, D. O'Dea, J. Paasch, T. Martin, L. Weng, J. Park, M. Fiala, M. Faham, and J. Wolf, *Deep sequencing reveals myeloma cells in peripheral blood in majority of multiple myeloma patients.* Clin Lymphoma Myeloma Leuk, 2014. **14**(2): p. 131-139 e1.

45. Manier, S., J. Park, M. Capelletti, M. Bustoros, S.S. Freeman, G. Ha, J. Rhoades, C.J. Liu, D. Huynh, S.C. Reed, G. Gydush, K.Z. Salem, D. Rotem, C. Freymond, A. Yosef, A. Perilla-Glen, L. Garderet, E.M. Van Allen, S. Kumar, J.C. Love, G. Getz, V.A. Adalsteinsson, and I.M. Ghobrial, *Whole-exome sequencing of cell-free DNA and circulating tumor cells in multiple myeloma.* Nat Commun, 2018. **9**(1): p. 1691.

46. Paiva, B., T. Paino, J.M. Sayagues, M. Garayoa, L. San-Segundo, M. Martin, I. Mota, M.L. Sanchez, P. Barcena, I. Aires-Mejia, L. Corchete, C. Jimenez, R. Garcia-Sanz, N.C. Gutierrez, E.M. Ocio, M.V. Mateos, M.B. Vidriales, A. Orfao, and J.F. San Miguel, *Detailed characterization of multiple myeloma circulating tumor cells shows unique phenotypic, cytogenetic, functional, and circadian distribution profile.* Blood, 2013. **122**(22): p. 3591-8.

47. Ledergor, G., A. Weiner, M. Zada, S.Y. Wang, Y.C. Cohen, M.E. Gatt, N. Snir, H. Magen, M. Koren-Michowitz, K. Herzog-Tzarfati, H. Keren-Shaul, C. Bornstein, R. Rotkopf, I. Yofe, E. David, V. Yellapantula, S. Kay, M. Salai, D. Ben Yehuda, A. Nagler, L. Shvidel, A. Orr-Urtreger, K.B. Halpern, S. Itzkovitz, O. Landgren, J. San-Miguel, B. Paiva, J.J. Keats, E. Papaemmanuil, I. Avivi, G.I. Barbash, A. Tanay, and

I. Amit, *Single cell dissection of plasma cell heterogeneity in symptomatic and asymptomatic myeloma.* Nat Med, 2018. **24**(12): p. 1867-1876.

48. Sanoja-Flores, L., J. Flores-Montero, N. Puig, T. Contreras-Sanfeliciano, R. Pontes, A. Corral-Mateos, O. Garcia-Sanchez, M. Diez-Campelo, R.J. Pessoa de Magalhaes, L. Garcia-Martin, J.M. Alonso-Alonso, A. Garcia-Mateo, C. Aguilar-Franco, J. Labrador, A. Barez-Garcia, A. Maiolino, B. Paiva, J. San Miguel, E. Sobral da Costa, M. Gonzalez, M.V. Mateos, B. Durie, J.J.M. van Dongen, and A. Orfao, *Blood monitoring of circulating tumor plasma cells by next generation flow in multiple myeloma after therapy.* Blood, 2019. **134**(24): p. 2218-2222.

49. Sanoja-Flores, L., J. Flores-Montero, J.J. Garces, B. Paiva, N. Puig, A. Garcia-Mateo, O. Garcia-Sanchez, A. Corral-Mateos, L. Burgos, E. Blanco, J. Hernandez-Martin, R. Pontes, M. Diez-Campelo, P. Millacoy, P. Rodriguez-Otero, F. Prosper, J. Merino, M.B. Vidriales, R. Garcia-Sanz, A. Romero, L. Palomera, R. Rios-Tamayo, M. Perez-Andres, J.F. Blanco, M. Gonzalez, J.J.M. van Dongen, B. Durie, M.V. Mateos, J. San-Miguel, A. Orfao, and c. EuroFlow, *Next generation flow for minimally-invasive blood characterization of MGUS and multiple myeloma at diagnosis based on circulating tumor plasma cells (CTPC).* Blood Cancer J, 2018. **8**(12): p. 117.

50. Gonsalves, W.I., W.G. Morice, V. Rajkumar, V. Gupta, M.M. Timm, A. Dispenzieri, F.K. Buadi, M.Q. Lacy, P.P. Singh, P. Kapoor, M.A. Gertz, and S.K. Kumar, *Quantification of clonal circulating plasma cells in relapsed multiple myeloma.* Br J Haematol, 2014. **167**(4): p. 500-5.

51. Dingli, D., G.S. Nowakowski, A. Dispenzieri, M.Q. Lacy, S.R. Hayman, S.V. Rajkumar, P.R. Greipp, M.R. Litzow, D.A. Gastineau, T.E. Witzig, and M.A. Gertz,

Flow cytometric detection of circulating myeloma cells before transplantation in patients with multiple myeloma: a simple risk stratification system. Blood, 2006. **107**(8): p. 3384-8.

52.   Puig, N., M.E. Sarasquete, A. Balanzategui, J. Martinez, B. Paiva, H. Garcia, S. Fumero, C. Jimenez, M. Alcoceba, M.C. Chillon, E. Sebastian, L. Marin, M.A. Montalban, M.V. Mateos, A. Oriol, L. Palomera, J. de la Rubia, M.B. Vidriales, J. Blade, J.J. Lahuerta, M. Gonzalez, J.F. Miguel, and R. Garcia-Sanz, *Critical evaluation of ASO RQ-PCR for minimal residual disease evaluation in multiple myeloma. A comparative analysis with flow cytometry.* Leukemia, 2014. **28**(2): p. 391-7.

53.   Berger, N., S. Kim-Schulze, and S. Parekh, *Minimal Residual Disease in Multiple Myeloma: Impact on Response Assessment, Prognosis and Tumor Heterogeneity.* Adv Exp Med Biol, 2018. **1100**: p. 141-159.

54.   van der Velden, V.H., G. Cazzaniga, A. Schrauder, J. Hancock, P. Bader, E.R. Panzer-Grumayer, T. Flohr, R. Sutton, H. Cave, H.O. Madsen, J.M. Cayuela, J. Trka, C. Eckert, L. Foroni, U. Zur Stadt, K. Beldjord, T. Raff, C.E. van der Schoot, J.J. van Dongen, and M.R.D.d.i.A.L.L. European Study Group on, *Analysis of minimal residual disease by Ig/TCR gene rearrangements: guidelines for interpretation of real-time quantitative PCR data.* Leukemia, 2007. **21**(4): p. 604-11.

55.   Sarasquete, M.E., R. Garcia-Sanz, D. Gonzalez, J. Martinez, G. Mateo, P. Martinez, J.M. Ribera, J.M. Hernandez, J.J. Lahuerta, A. Orfao, M. Gonzalez, and J.F. San Miguel, *Minimal residual disease monitoring in multiple myeloma: a comparison*

between allelic-specific oligonucleotide real-time quantitative polymerase chain reaction and flow cytometry. Haematologica, 2005. **90**(10): p. 1365-72.

56.   Yao, Q., Y. Bai, A. Orfao, and C.S. Chim, *Standardized Minimal Residual Disease Detection by Next-Generation Sequencing in Multiple Myeloma.* Front Oncol, 2019. **9**: p. 449.

57.   Drandi, D., L. Kubiczkova-Besse, S. Ferrero, N. Dani, R. Passera, B. Mantoan, M. Gambella, L. Monitillo, E. Saraci, P. Ghione, E. Genuardi, D. Barbero, P. Omede, D. Barberio, R. Hajek, U. Vitolo, A. Palumbo, S. Cortelazzo, M. Boccadoro, G. Inghirami, and M. Ladetto, *Minimal Residual Disease Detection by Droplet Digital PCR in Multiple Myeloma, Mantle Cell Lymphoma, and Follicular Lymphoma: A Comparison with Real-Time PCR.* J Mol Diagn, 2015. **17**(6): p. 652-60.

58.   Takamatsu, H., *Comparison of Minimal Residual Disease Detection by Multiparameter Flow Cytometry, ASO-qPCR, Droplet Digital PCR, and Deep Sequencing in Patients with Multiple Myeloma Who Underwent Autologous Stem Cell Transplantation.* J Clin Med, 2017. **6**(10).

59.   Langerhorst, P., A.B. Brinkman, M.M. VanDuijn, H. Wessels, P. Groenen, I. Joosten, A.J. van Gool, J. Gloerich, B. Scheijen, and J.F.M. Jacobs, *Clonotypic Features of Rearranged Immunoglobulin Genes Yield Personalized Biomarkers for Minimal Residual Disease Monitoring in Multiple Myeloma.* Clin Chem, 2021.

60.   Zajec, M., J.F.M. Jacobs, P. Groenen, C.M. de Kat Angelino, C. Stingl, T.M. Luider, Y.B. De Rijke, and M.M. VanDuijn, *Development of a Targeted Mass-Spectrometry Serum Assay To Quantify M-Protein in the Presence of Therapeutic Monoclonal Antibodies.* J Proteome Res, 2018. **17**(3): p. 1326-1333.

61.   Barnidge, D.R., R.C. Tschumper, J.D. Theis, M.R. Snyder, D.F. Jelinek, J.A. Katzmann, A. Dispenzieri, and D.L. Murray, *Monitoring M-proteins in patients with multiple myeloma using heavy-chain variable region clonotypic peptides and LC-MS/MS.* J Proteome Res, 2014. **13**(4): p. 1905-10.

62.   Eveillard, M., E. Rustad, M. Roshal, Y. Zhang, A. Ciardiello, N. Korde, M. Hultcrantz, S. Lu, U. Shah, H. Hassoun, E. Smith, A. Lesokhin, S. Mailankody, O. Landgren, and K. Thoren, *Comparison of MALDI-TOF mass spectrometry analysis of peripheral blood and bone marrow-based flow cytometry for tracking measurable residual disease in patients with multiple myeloma.* Br J Haematol, 2020. **189**(5): p. 904-907.

63.   Barnidge, D.R., S. Dasari, C.M. Botz, D.H. Murray, M.R. Snyder, J.A. Katzmann, A. Dispenzieri, and D.L. Murray, *Using mass spectrometry to monitor monoclonal immunoglobulins in patients with a monoclonal gammopathy.* J Proteome Res, 2014. **13**(3): p. 1419-27.

64.   Bergen, H.R., 3rd, S. Dasari, A. Dispenzieri, J.R. Mills, M. Ramirez-Alvarado, R.C. Tschumper, D.F. Jelinek, D.R. Barnidge, and D.L. Murray, *Clonotypic Light Chain Peptides Identified for Monitoring Minimal Residual Disease in Multiple Myeloma without Bone Marrow Aspiration.* Clin Chem, 2016. **62**(1): p. 243-51.

65.   Murray, D.L., N. Puig, S. Kristinsson, S.Z. Usmani, A. Dispenzieri, G. Bianchi, S. Kumar, W.J. Chng, R. Hajek, B. Paiva, A. Waage, S.V. Rajkumar, and B. Durie, *Mass spectrometry for the evaluation of monoclonal proteins in multiple myeloma and related disorders: an International Myeloma Working Group Mass Spectrometry Committee Report.* Blood Cancer J, 2021. **11**(2): p. 24.

66. Tapia-Alveal, C., T.R. Olsen, and T.S. Worgall, *Personalized immunoglobulin aptamers for detection of multiple myeloma minimal residual disease in serum.* Commun Biol, 2020. **3**(1): p. 781.

67. Mills, J.R., D.R. Barnidge, A. Dispenzieri, and D.L. Murray, *High sensitivity blood-based M-protein detection in sCR patients with multiple myeloma.* Blood Cancer J, 2017. **7**(8): p. e590.

68. Derman, B.A., A.T. Stefka, K. Jiang, A. McIver, T. Kubicki, J.K. Jasielec, and A.J. Jakubowiak, *Measurable residual disease assessed by mass spectrometry in peripheral blood in multiple myeloma in a phase II trial of carfilzomib, lenalidomide, dexamethasone and autologous stem cell transplantation.* Blood Cancer J, 2021. **11**(2): p. 19.

69. Medina, A., N. Puig, J. Flores-Montero, C. Jimenez, M.E. Sarasquete, M. Garcia-Alvarez, I. Prieto-Conde, C. Chillon, M. Alcoceba, N.C. Gutierrez, A. Oriol, L. Rosinol, J. Blade, M. Gironella, M.T. Hernandez, V. Gonzalez-Calle, M.T. Cedena, B. Paiva, J.F. San-Miguel, J.J. Lahuerta, M.V. Mateos, J. Martinez-Lopez, A. Orfao, M. Gonzalez, and R. Garcia-Sanz, *Comparison of next-generation sequencing (NGS) and next-generation flow (NGF) for minimal residual disease (MRD) assessment in multiple myeloma.* Blood Cancer J, 2020. **10**(10): p. 108.

70. Kriegsmann, K., M. Hundemer, N. Hofmeister-Mielke, P. Reichert, C.P. Manta, M.H.S. Awwad, S. Sauer, U. Bertsch, B. Besemer, R. Fenk, M. Hanel, M. Munder, K.C. Weisel, I.W. Blau, A. Neubauer, C. Muller-Tidow, M.S. Raab, H. Goldschmidt, S. Huhn, and G. For The German-Speaking Myeloma Multicenter Group,

Comparison of NGS and MFC Methods: Key Metrics in Multiple Myeloma MRD Assessment. Cancers (Basel), 2020. **12**(8).

71.   Wu, D., A. Sherwood, J.R. Fromm, S.S. Winter, K.P. Dunsmore, M.L. Loh, H.A. Greisman, D.E. Sabath, B.L. Wood, and H. Robins, *High-throughput sequencing detects minimal residual disease in acute T lymphoblastic leukemia.* Sci Transl Med, 2012. **4**(134): p. 134ra63.

72.   Appenzeller, S., C. Gilissen, J. Rijntjes, B.B. Tops, A. Kastner-van Raaij, K.M. Hebeda, L. Nissen, B.E. Dutilh, J.H. van Krieken, and P.J. Groenen, *Immunoglobulin rearrangement analysis from multiple lesions in the same patient using next-generation sequencing.* Histopathology, 2015. **67**(6): p. 843-58.

73.   Rajala, H.L., T. Olson, M.J. Clemente, S. Lagstrom, P. Ellonen, T. Lundan, D.E. Hamm, S.A. Zaman, J.M. Lopez Marti, E.I. Andersson, A. Jerez, K. Porkka, J.P. Maciejewski, T.P. Loughran, and S. Mustjoki, *The analysis of clonal diversity and therapy responses using STAT3 mutations as a molecular marker in large granular lymphocytic leukemia.* Haematologica, 2015. **100**(1): p. 91-9.

74.   Schumacher, J.A., E.J. Duncavage, T.L. Mosbruger, P.M. Szankasi, and T.W. Kelley, *A comparison of deep sequencing of TCRG rearrangements vs traditional capillary electrophoresis for assessment of clonality in T-Cell lymphoproliferative disorders.* Am J Clin Pathol, 2014. **141**(3): p. 348-59.

75.   Faham, M., J. Zheng, M. Moorhead, V.E. Carlton, P. Stow, E. Coustan-Smith, C.H. Pui, and D. Campana, *Deep-sequencing approach for minimal residual disease detection in acute lymphoblastic leukemia.* Blood, 2012. **120**(26): p. 5173-80.

76.   Faham, M.W., Thomas, *Monitoring health and disease status using clonotype profiles*. 2011, Adaptive Biotechnologies corp: United States.

77.   Corporation, A.B., *clonoSEQ® Assay Technical Information*. 2019.

78.   Drilon, A., L. Wang, M.E. Arcila, S. Balasubramanian, J.R. Greenbowe, J.S. Ross, P. Stephens, D. Lipson, V.A. Miller, M.G. Kris, M. Ladanyi, and N.A. Rizvi, *Broad, Hybrid Capture-Based Next-Generation Sequencing Identifies Actionable Genomic Alterations in Lung Adenocarcinomas Otherwise Negative for Such Alterations by Other Genomic Testing Approaches.* Clin Cancer Res, 2015. **21**(16): p. 3631-9.

79.   Xie, J., X. Lu, X. Wu, X. Lin, C. Zhang, X. Huang, Z. Chang, X. Wang, C. Wen, X. Tang, M. Shi, Q. Zhan, H. Chen, X. Deng, C. Peng, H. Li, Y. Fang, Y. Shao, and B. Shen, *Capture-based next-generation sequencing reveals multiple actionable mutations in cancer patients failed in traditional testing.* Mol Genet Genomic Med, 2016. **4**(3): p. 262-72.

80.   Roschewski, M., D. Rossi, D.M. Kurtz, A.A. Alizadeh, and W.H. Wilson, *Circulating Tumor DNA in Lymphoma: Principles and Future Directions.* Blood Cancer Discov, 2022. **3**(1): p. 5-15.

81.   Bohers, E., P.J. Viailly, S. Dubois, P. Bertrand, C. Maingonnat, S. Mareschal, P. Ruminy, J.M. Picquenot, C. Bastard, F. Desmots, T. Fest, K. Leroy, H. Tilly, and F. Jardin, *Somatic mutations of cell-free circulating DNA detected by next-generation sequencing reflect the genetic changes in both germinal center B-cell-like and activated B-cell-like diffuse large B-cell lymphomas at the time of diagnosis.* Haematologica, 2015. **100**(7): p. e280-4.

82.   Camus, V., F. Jardin, and H. Tilly, *The value of liquid biopsy in diagnosis and monitoring of diffuse large b-cell lymphoma: recent developments and future potential.* Expert Rev Mol Diagn, 2017. **17**(6): p. 557-566.

83.   Clark, T.A., J.H. Chung, M. Kennedy, J.D. Hughes, N. Chennagiri, D.S. Lieber, B. Fendler, L. Young, M. Zhao, M. Coyne, V. Breese, G. Young, A. Donahue, D. Pavlick, A. Tsiros, T. Brennan, S. Zhong, T. Mughal, M. Bailey, J. He, S. Roels, G.M. Frampton, J.M. Spoerke, S. Gendreau, M. Lackner, E. Schleifman, E. Peters, J.S. Ross, S.M. Ali, V.A. Miller, J.P. Gregg, P.J. Stephens, A. Welsh, G.A. Otto, and D. Lipson, *Analytical Validation of a Hybrid Capture-Based Next-Generation Sequencing Clinical Assay for Genomic Profiling of Cell-Free Circulating Tumor DNA.* J Mol Diagn, 2018. **20**(5): p. 686-702.

84.   Corcoran, R.B. and B.A. Chabner, *Application of Cell-free DNA Analysis to Cancer Treatment.* N Engl J Med, 2018. **379**(18): p. 1754-1765.

85.   Kis, O., R. Kaedbey, S. Chow, A. Danesh, M. Dowar, T. Li, Z. Li, J. Liu, M. Mansour, E. Masih-Khan, T. Zhang, S.V. Bratman, A.M. Oza, S. Kamel-Reid, S. Trudel, and T.J. Pugh, *Circulating tumour DNA sequence analysis as an alternative to multiple myeloma bone marrow aspirates.* Nat Commun, 2017. **8**(1): p. 15086.

86.   Scherer, F., D.M. Kurtz, A.M. Newman, H. Stehr, A.F. Craig, M.S. Esfahani, A.F. Lovejoy, J.J. Chabon, D.M. Klass, C.L. Liu, L. Zhou, C. Glover, B.C. Visser, G.A. Poultsides, R.H. Advani, L.S. Maeda, N.K. Gupta, R. Levy, R.S. Ohgami, C.A. Kunder, M. Diehn, and A.A. Alizadeh, *Distinct biological subtypes and patterns of genome evolution in lymphoma revealed by circulating tumor DNA.* Sci Transl Med, 2016. **8**(364): p. 364ra155.

87.   Kwapisz, D., *The first liquid biopsy test approved. Is it a new era of mutation testing for non-small cell lung cancer?* Ann Transl Med, 2017. **5**(3): p. 46.

88.   Oberle, A., A. Brandt, M. Voigtlaender, B. Thiele, J. Radloff, A. Schulenkorf, M. Alawi, N. Akyuz, M. Marz, C.T. Ford, A. Krohn-Grimberghe, and M. Binder, *Monitoring multiple myeloma by next-generation sequencing of V(D)J rearrangements from circulating myeloma cells and cell-free myeloma DNA.* Haematologica, 2017. **102**(6): p. 1105-1111.

89.   Biancon, G., S. Gimondi, A. Vendramin, C. Carniti, and P. Corradini, *Noninvasive Molecular Monitoring in Multiple Myeloma Patients Using Cell-Free Tumor DNA: A Pilot Study.* J Mol Diagn, 2018. **20**(6): p. 859-870.

90.   Mazzotti, C., L. Buisson, S. Maheo, A. Perrot, M.L. Chretien, X. Leleu, C. Hulin, S. Manier, B. Hebraud, M. Roussel, L. Do Souto, M. Attal, H. Avet-Loiseau, and J. Corre, *Myeloma MRD by deep sequencing from circulating tumor DNA does not correlate with results obtained in the bone marrow.* Blood Adv, 2018. **2**(21): p. 2811-2813.

91.   Rustad, E.H., E. Coward, E.R. Skytoen, K. Misund, T. Holien, T. Standal, M. Borset, V. Beisvag, O. Myklebost, L.A. Meza-Zepeda, H.Y. Dai, A. Sundan, and A. Waage, *Monitoring multiple myeloma by quantification of recurrent mutations in serum.* Haematologica, 2017. **102**(7): p. 1266-1272.

92.   Li, Q., H.J. Huang, J. Ma, Y. Wang, Z. Cao, G. Karlin-Neumann, F. Janku, and Z. Liu, *RAS/RAF mutations in tumor samples and cell-free DNA from plasma and bone marrow aspirates in multiple myeloma patients.* J Cancer, 2020. **11**(12): p. 3543-3550.

93. Cherng, H.J., R. Sun, B. Sugg, R. Irwin, H. Yang, C.C. Le, Q. Deng, L.E. Fayad, N.H. Fowler, S. Parmar, R.E. Steiner, F.B. Hagemeister, R. Nair, H.J. Lee, M.A. Rodriguez, F. Samaniego, S.P. Iyer, C.R. Flowers, L. Wang, L.J. Nastoupil, S.S. Neelapu, S. Ahmed, P. Strati, M.R. Green, and J.R. Westin, *Risk assessment with low pass whole genome sequencing of cell free DNA before CD19 CAR T-cells for large B-cell lymphoma.* Blood, 2022.

94. Waldschmidt, J.M., A.J. Yee, T. Vijaykumar, R.A. Pinto, J. Frede, P. Anand, G. Bianchi, G. Guo, S. Potdar, C. Seifer, M.S. Nair, A. Kokkalis, J.A. Kloeber, S. Shapiro, L. Budano, M. Mann, R. Friedman, B. Lipe, E. Campagnaro, E.K. O'Donnell, C.Z. Zhang, J.P. Laubach, N.C. Munshi, P.G. Richardson, K.C. Anderson, N.S. Raje, B. Knoechel, and J.G. Lohr, *Cell-free DNA for the detection of emerging treatment failure in relapsed/ refractory multiple myeloma.* Leukemia, 2022.

95. Gaudin, M. and C. Desnues, *Hybrid Capture-Based Next Generation Sequencing and Its Application to Human Infectious Diseases.* Front Microbiol, 2018. **9**: p. 2924.

96. Newman, A.M., S.V. Bratman, J. To, J.F. Wynne, N.C. Eclov, L.A. Modlin, C.L. Liu, J.W. Neal, H.A. Wakelee, R.E. Merritt, J.B. Shrager, B.W. Loo, Jr., A.A. Alizadeh, and M. Diehn, *An ultrasensitive method for quantitating circulating tumor DNA with broad patient coverage.* Nat Med, 2014. **20**(5): p. 548-54.

97. Kurtz, D.M., F. Scherer, M.C. Jin, J. Soo, A.F.M. Craig, M.S. Esfahani, J.J. Chabon, H. Stehr, C.L. Liu, R. Tibshirani, L.S. Maeda, N.K. Gupta, M.S. Khodadoust, R.H. Advani, R. Levy, A.M. Newman, U. Duhrsen, A. Huttmann, M. Meignan, R.O. Casasnovas, J.R. Westin, M. Roschewski, W.H. Wilson, G. Gaidano, D. Rossi, M. Diehn, and A.A. Alizadeh, *Circulating Tumor DNA Measurements As Early Outcome*

Predictors in Diffuse Large B-Cell Lymphoma. J Clin Oncol, 2018. **36**(28): p. 2845-2853.

98.   Yellapantula, V., M. Hultcrantz, E.H. Rustad, E. Wasserman, D. Londono, R. Cimera, A. Ciardiello, H. Landau, T. Akhlaghi, S. Mailankody, M. Patel, J.S. Medina-Martinez, J.E. Arango Ossa, M.F. Levine, N. Bolli, F. Maura, A. Dogan, E. Papaemmanuil, Y. Zhang, and O. Landgren, *Comprehensive detection of recurring genomic abnormalities: a targeted sequencing approach for multiple myeloma.* Blood Cancer J, 2019. **9**(12): p. 101.

99.   Jimenez, C., M. Jara-Acevedo, L.A. Corchete, D. Castillo, G.R. Ordonez, M.E. Sarasquete, N. Puig, J. Martinez-Lopez, M.I. Prieto-Conde, M. Garcia-Alvarez, M.C. Chillon, A. Balanzategui, M. Alcoceba, A. Oriol, L. Rosinol, L. Palomera, A.I. Teruel, J.J. Lahuerta, J. Blade, M.V. Mateos, A. Orfao, J.F. San Miguel, M. Gonzalez, N.C. Gutierrez, and R. Garcia-Sanz, *A Next-Generation Sequencing Strategy for Evaluating the Most Common Genetic Abnormalities in Multiple Myeloma.* J Mol Diagn, 2017. **19**(1): p. 99-106.

100.   Astle, J.M., M.L. Xu, T. Friedman, and E. Brown, *Limitations of poor bone marrow aspirations (for an accurate diagnosis) despite the multimodal analytical era: A longitudinal retrospective study.* Am J Hematol, 2017. **92**(10): p. E600-E602.

101.   Mithraprabhu, S., T. Khong, M. Ramachandran, A. Chow, D. Klarica, L. Mai, S. Walsh, D. Broemeling, A. Marziali, M. Wiggin, J. Hocking, A. Kalff, B. Durie, and A. Spencer, *Circulating tumour DNA analysis demonstrates spatial mutational heterogeneity that coincides with disease relapse in myeloma.* Leukemia, 2017. **31**(8): p. 1695-1705.

102. Costa, L.J., B.A. Derman, S. Bal, S. Sidana, S. Chhabra, R. Silbermann, J.C. Ye, G. Cook, R.F. Cornell, S.A. Holstein, Q. Shi, J. Omel, N.S. Callander, W.J. Chng, V. Hungria, A. Maiolino, E. Stadtmauer, S. Giralt, M. Pasquini, A.J. Jakubowiak, G.J. Morgan, A. Krishnan, G.H. Jackson, M. Mohty, M.V. Mateos, M.A. Dimopoulos, T. Facon, A. Spencer, J.S. Miguel, P. Hari, S.Z. Usmani, S. Manier, P. McCarthy, S. Kumar, F. Gay, and B. Paiva, *International harmonization in performing and reporting minimal residual disease assessment in multiple myeloma trials.* Leukemia, 2021. **35**(1): p. 18-30.

103. van Dongen, J.J., V.H. van der Velden, M. Bruggemann, and A. Orfao, *Minimal residual disease diagnostics in acute lymphoblastic leukemia: need for sensitive, fast, and standardized technologies.* Blood, 2015. **125**(26): p. 3996-4009.

104. Rustad, E.H. and E.M. Boyle, *Monitoring minimal residual disease in the bone marrow using next generation sequencing.* Best Pract Res Clin Haematol, 2020. **33**(1): p. 101149.

105. Jovanovic, B.D. and P.S. Levy, *A Look at the Rule of Three.* The American Statistician, 1997. **51**(2): p. 137-139.

106. Hansen, M.H., O. Cedile, T.S. Larsen, N. Abildgaard, and C.G. Nyvold, *Perspective: Sensitive detection of residual lymphoproliferative disease by clonal gene rearrangements and NGS - How low can you go?* Exp Hematol, 2021.

107. Costello, M., M. Fleharty, J. Abreu, Y. Farjoun, S. Ferriera, L. Holmes, B. Granger, L. Green, T. Howd, T. Mason, G. Vicente, M. Dasilva, W. Brodeur, T. DeSmet, S. Dodge, N.J. Lennon, and S. Gabriel, *Characterization and remediation of sample*

index swaps by non-redundant dual indexing on massively parallel sequencing platforms. BMC Genomics, 2018. **19**(1): p. 332.

108.   Stoler, N. and A. Nekrutenko, *Sequencing error profiles of Illumina sequencing instruments.* NAR Genom Bioinform, 2021. **3**(1): p. lqab019.

109.   Potapov, V. and J.L. Ong, *Examining Sources of Error in PCR by Single-Molecule Sequencing.* PLoS One, 2017. **12**(1): p. e0169774.

110.   Miner, B.E., R.J. Stoger, A.F. Burden, C.D. Laird, and R.S. Hansen, *Molecular barcodes detect redundancy and contamination in hairpin-bisulfite PCR.* Nucleic Acids Res, 2004. **32**(17): p. e135.

111.   McCloskey, M.L., R. Stoger, R.S. Hansen, and C.D. Laird, *Encoding PCR products with batch-stamps and barcodes.* Biochem Genet, 2007. **45**(11-12): p. 761-7.

112.   Kinde, I., J. Wu, N. Papadopoulos, K.W. Kinzler, and B. Vogelstein, *Detection and quantification of rare mutations with massively parallel sequencing.* Proc Natl Acad Sci U S A, 2011. **108**(23): p. 9530-5.

113.   Schmitt, M.W., S.R. Kennedy, J.J. Salk, E.J. Fox, J.B. Hiatt, and L.A. Loeb, *Detection of ultra-rare mutations by next-generation sequencing.* Proc Natl Acad Sci U S A, 2012. **109**(36): p. 14508-13.

114.   Kennedy, S.R., M.W. Schmitt, E.J. Fox, B.F. Kohrn, J.J. Salk, E.H. Ahn, M.J. Prindle, K.J. Kuong, J.C. Shen, R.A. Risques, and L.A. Loeb, *Detecting ultralow-frequency mutations by Duplex Sequencing.* Nat Protoc, 2014. **9**(11): p. 2586-606.

115.   Newman, A.M., A.F. Lovejoy, D.M. Klass, D.M. Kurtz, J.J. Chabon, F. Scherer, H. Stehr, C.L. Liu, S.V. Bratman, C. Say, L. Zhou, J.N. Carter, R.B. West, G.W. Sledge, J.B. Shrager, B.W. Loo, Jr., J.W. Neal, H.A. Wakelee, M. Diehn, and A.A. Alizadeh,

Integrated digital error suppression for improved detection of circulating tumor DNA. Nat Biotechnol, 2016. **34**(5): p. 547-555.

116.   Kurtz, D.M., J. Soo, L. Co Ting Keh, S. Alig, J.J. Chabon, B.J. Sworder, A. Schultz, M.C. Jin, F. Scherer, A. Garofalo, C.W. Macaulay, E.G. Hamilton, B. Chen, M. Olsen, J.G. Schroers-Martin, A.F.M. Craig, E.J. Moding, M.S. Esfahani, C.L. Liu, U. Duhrsen, A. Huttmann, R.O. Casasnovas, J.R. Westin, M. Roschewski, W.H. Wilson, G. Gaidano, D. Rossi, M. Diehn, and A.A. Alizadeh, *Enhanced detection of minimal residual disease by targeted sequencing of phased variants in circulating tumor DNA.* Nat Biotechnol, 2021. **39**(12): p. 1537-1547.

117.   Wong, S.W., N. Shah, G. Ledergor, T. Martin, J. Wolf, A.M. Shui, C.Y. Huang, and J. Martinez-Lopez, *Early Dynamics and Depth of Response in Multiple Myeloma Patients Treated With BCMA CAR-T Cells.* Front Oncol, 2021. **11**: p. 783703.

118.   Deng, Q., G. Han, N. Puebla-Osorio, M.C.J. Ma, P. Strati, B. Chasen, E. Dai, M. Dang, N. Jain, H. Yang, Y. Wang, S. Zhang, R. Wang, R. Chen, J. Showell, S. Ghosh, S. Patchva, Q. Zhang, R. Sun, F. Hagemeister, L. Fayad, F. Samaniego, H.C. Lee, L.J. Nastoupil, N. Fowler, R. Eric Davis, J. Westin, S.S. Neelapu, L. Wang, and M.R. Green, *Characteristics of anti-CD19 CAR T cell infusion products associated with efficacy and toxicity in patients with large B cell lymphomas.* Nat Med, 2020. **26**(12): p. 1878-1887.

119.   Lagana, A., D. Perumal, D. Melnekoff, B. Readhead, B.A. Kidd, V. Leshchenko, P.Y. Kuo, J. Keats, M. DeRome, J. Yesil, D. Auclair, S. Lonial, A. Chari, H.J. Cho, B. Barlogie, S. Jagannath, J.T. Dudley, and S. Parekh, *Integrative network analysis*

identifies novel drivers of pathogenesis and progression in newly diagnosed multiple myeloma. Leukemia, 2018. **32**(1): p. 120-130.

120. Karczewski, K.J., B. Weisburd, B. Thomas, M. Solomonson, D.M. Ruderfer, D. Kavanagh, T. Hamamsy, M. Lek, K.E. Samocha, B.B. Cummings, D. Birnbaum, C. The Exome Aggregation, M.J. Daly, and D.G. MacArthur, *The ExAC browser: displaying reference data information from over 60 000 exomes.* Nucleic Acids Res, 2017. **45**(D1): p. D840-D845.

121. Ng, S.B., E.H. Turner, P.D. Robertson, S.D. Flygare, A.W. Bigham, C. Lee, T. Shaffer, M. Wong, A. Bhattacharjee, E.E. Eichler, M. Bamshad, D.A. Nickerson, and J. Shendure, *Targeted capture and massively parallel sequencing of 12 human exomes.* Nature, 2009. **461**(7261): p. 272-6.

122. Sherry, S.T., M.H. Ward, M. Kholodov, J. Baker, L. Phan, E.M. Smigielski, and K. Sirotkin, *dbSNP: the NCBI database of genetic variation.* Nucleic Acids Res, 2001. **29**(1): p. 308-11.

123. Deshpande, S., R.G. Tytarenko, Y. Wang, E.M. Boyle, C. Ashby, C.D. Schinke, S. Thanendrarajan, M. Zangari, F. Zhan, F.E. Davies, G.J. Morgan, F. van Rhee, and B.A. Walker, *Monitoring treatment response and disease progression in myeloma with circulating cell-free DNA.* Eur J Haematol, 2021. **106**(2): p. 230-240.

124. Husain, H., V.O. Melnikova, K. Kosco, B. Woodward, S. More, S.C. Pingle, E. Weihe, B.H. Park, M. Tewari, M.G. Erlander, E. Cohen, S.M. Lippman, and R. Kurzrock, *Monitoring Daily Dynamics of Early Tumor Response to Targeted Therapy by Detecting Circulating Tumor DNA in Urine.* Clin Cancer Res, 2017. **23**(16): p. 4716-4723.

12 <u>Vita</u>

Russell Irwin was born in New Mexico in 1998 to a military family. After a brief time in California, the family settled in San Antonio, TX in 2004. For achieving the highest grade in his sixth-grade science class, he was awarded a pair of orange lab goggles, an award which would prove to be foretelling. He attended Health Careers High School and became interested in medicine and the complex interplay between the fine molecular and human sides of medicine. During this time, he chose to pursue medicine as a career after working in ORs and, during one memorable rotation, comforting newborns suffering from neonatal abstinence syndrome- opiate withdrawal. It was also here that he was trained as a pharmacy technician.

He attended Oklahoma State University in Stillwater, graduating *cum laude* with a Bachelor of Science in Agricultural Sciences and Natural Resources, majoring in Biochemistry and Molecular Biology, with an Honors College degree, in 2020. While at OSU, he was mentored by Dr. John Gustafson and William Johnson, whose research into antimicrobial resistance of the nosocomial pathogen *Elizabethkingia* inspired his own decision to pursue research. Shortly after the final aims of this research were stymied by the coronavirus pandemic, Irwin moved to Houston, enrolled at the University of Texas MD Anderson Cancer Center UTHealth Graduate School of Biomedical Sciences, and joined Michael Green's lab at MD Anderson Cancer Center in order to investigate the ability of hybrid capture of cfDNA to monitor multiple myeloma.

Contact info: Russell.m.irwin@gmail.com

Linkedin: www.linkedin.com/in/russell-irwin-018254144